Winter 2011

Marine atmospheric influences on trace gas observations and transport during the ICARTT 2004 campaign

Shannon R. Davis
University of New Hampshire, Durham

MARINE ATMOSPHERIC INFLUENCES ON TRACE GAS OBSERVATIONS AND TRANSPORT DURING THE ICARTT 2004 CAMPAIGN

BY

SHANNON R. DAVIS
BS and BA, College of William and Mary, 1995
MS, Florida State University, 2002

DISSERTATION

Submitted to the University of New Hampshire

in Partial Fulfillment of

the Requirements for the Degree of

Doctor of Philosophy
in
Earth and Environmental Sciences
December, 2011

UMI Number: 3500781

UMI®

Dissertation Publishing

ProQuest®
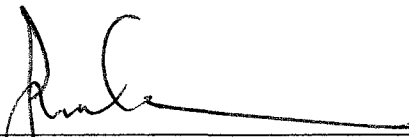
This dissertation has been examined and approved.
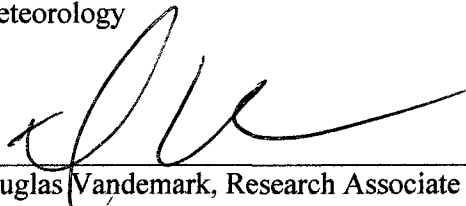
_____
Dissertation Director, Robert W. Talbot, Adjunct
Research Professor of Atmospheric Chemistry

_____
Huiting Mao, Adjunct Research Associate
Professor of Atmospheric Chemistry

_____
Samuel T. Miller, Associate Professor of
Meteorology

_____
Douglas Vandemark, Research Associate
Professor of Earth, Ocean and Space

_____
Bobby Braswell, Senior Research Scientist of
Applied Geosolutions, LLC

_____
Date

DEDICATION

For Bob and Diane, who held me up high in the Montana sky when I was small, carried me on their shoulders along the banks of the Swan River, and throughout the rest of their lives, showing me that no dream was ever out of reach and that it was always that much richer for being shared. This was for you Mom and Dad.

For my dearest friend and most faithful companion, Allegro, who never left my side, reminded me to always appreciate the subtler sides of life, and who imparted his art of making any and every day an adventure.

And for the love of life, my wife Xujing, who always gave me hope, made each step mean more, and who always finds ways to brighten my heart. There is no one else I would build a new world with, so this was for you too lao peu, with all my heart. Wuh I Ni.

ACKNOWLEDGEMENTS

TABLE OF CONTENTS

LIST OF TABLES

LIST OF FIGURES

ABSTRACT

MARINE ATMOSPHERIC INFLUENCES ON TRACE GAS OBSERVATIONS AND TRANSPORT DURING THE ICARTT 2004 CAMPAIGN

by

Shannon R. Davis

University of New Hampshire, December, 2011

The transport of pollutant trace gases and aerosols above coastal waters is of eminent importance to air quality and global climate processes. The research presented in this dissertation is a two-part investigation of this transport as observed during the ICARTT campaign, with focus devoted to the transit and evolution of trace gases in the lower marine atmosphere above the Gulf of Maine (GOM) and western North Atlantic Ocean. Part I advances a quasi-lagrangian case study of a plume emanating from the New York City source region. In this, analysis of airborne intercepts of the plume captured its transformation from a polluted airmass within a residual layer, to a well defined flow maintained within a stable internal boundary layer (SIBL). The SIBL was defined by sharp gradients in moisture, temperature and wind speed, and persisted throughout the NYC plume's transit. Further investigation showed that the SIBL measurably influenced trace gas variability and evolution. Despite its low altitude, the

SIBL strongly inhibited surface interactions, thus limiting removal processes. Pronounced vertical shear in wind speed generated frequent instances of Kelvin-Helmholtz instability and turbulence within the plume layer. This resulted in a high degree of spatial variability in mixing ratios observed within the plume, enhanced mixing, and contributions to its overall transit. Surface observations during the plume passage recorded pollutant mixing ratios equaling the most extreme measured that summer, a fact that motivated the further investigation of the SIBL pursued in Part II. In this, an extended analysis of the coastal SIBL was presented in the context of the entire campaign period. The SIBL was detected in the majority of low-altitude flights over the GOM, with its thickness varying significantly with fetch during the day and to a lesser extent at night. Nocturnal observations revealed the periodic detection of a low level jet within the SIBL. Overall, SIBL heights for both time period were higher than the predicted values determined from SIBL relationships established in related studies, suggesting that additional parameters like turbulent fluxes or surface roughness are required to determine SIBL development in the region.

CHAPTER 1: INTRODUCTION

1.1 General Introduction

The atmosphere above the North Atlantic Ocean is a principle pathway for the outflow of trace gases and aerosols from the United States and Canada. Recent estimates suggest that these emissions contribute between 15-23% to the world-wide inventory of traces gas pollutants which impinge on surface air quality downwind as well as negatively perturb large scale radiative processes that influence the global climate (Cooper et al., 2004). Three primary atmospheric mechanisms facilitate this continental outflow. Two of these mechanisms, deep convection and warm conveyor belt transport, are tied to the venting of pollutants high (>3km) into the upper troposphere where they are advected across the Atlantic on 3-5 day timescales (Stohl et al., 2001). The third mechanism and focus of the research presented here is low level outflow (LLO). This is achieved at lower altitudes (<3km), where coastal dynamics and the structure of the lower marine troposphere play an essential role in arranging the transport of polluted continental air in thin layers within or just above the marine boundary layer. This form of outflow is commonly observed across the Western North Atlantic, transiting in 5-8 day time spans (Owen et al. 2006) and often within pathways that pass through the Gulf of Maine (GOM) region.

1
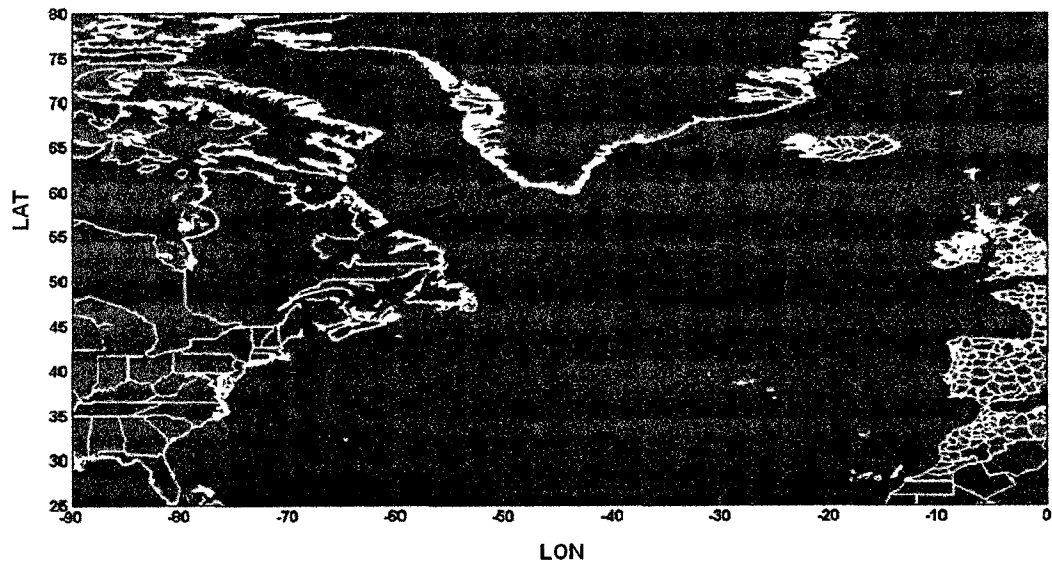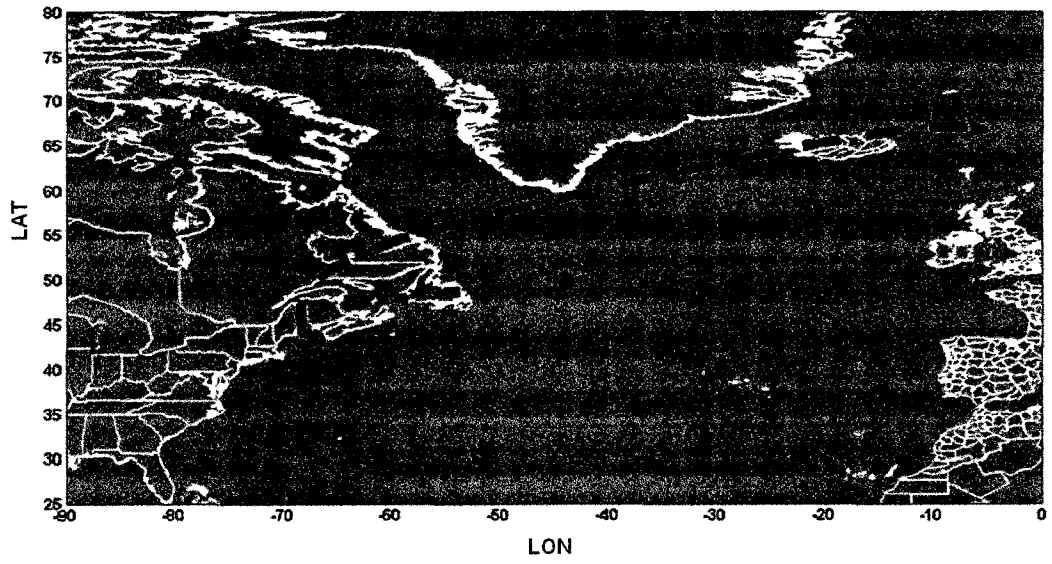
Figure 1.1. Schematic of North American transatlantic outflow pathways prevalent in

a) summer and b) winter with upper tropospheric pathways indicated in blue and lower

tropospheric ones in red.

For both upper and lower level forms of outflow, previous work has established the prominent routes followed by polluted plumes as they cross the North Atlantic. Key among these was the 15-year climatology of lagrangian model simulation study conducted by Eckhardt et al. (2003), which revealed a strong similarity between the upper and lower tropospheric patterns, as well as a slight southward shift between summer and winter seasons. For both summer and winter seasons it is evident that each form of outflow follows the prevailing storm track across the Atlantic with a slight north to south modulation in the lower track between winter and summer. Importantly, the northeastern U.S. and in particular the GOM, can be seen to play a role in the low level transport in both seasons. A schematic of these outflow patterns is shown in Figure 1.1. However, what is not apparent from the figure is that the GOM itself is a downwind receptor region for continental and coastal plumes. This is an essential aspect to its importance and role in the LLO process.

To some extent, this was discussed in a study by Angevine et al (2004), who related that most polluted plumes in the GOM region are transported instead of being formed locally. A clear example of this can be seen in the MODIS satellite imagery from July 20, 2004 presented in Figure 1.2, which captures the arrival of several diverse incoming polluted airmasses as well as low altitude outflow into the Western North Atlantic. Specifically visible in this satellite image are a Canadian wildfire/biomass burning plume described by Warneke et al. (2006), a low level coastal plume from the NYC source region (Davis et al. 2011, Real et al. 2008, Mao et al. 2006), as well as an accumulation of aged anthropogenic emissions (Millet et al. 2006, Neumann et al. 2006).
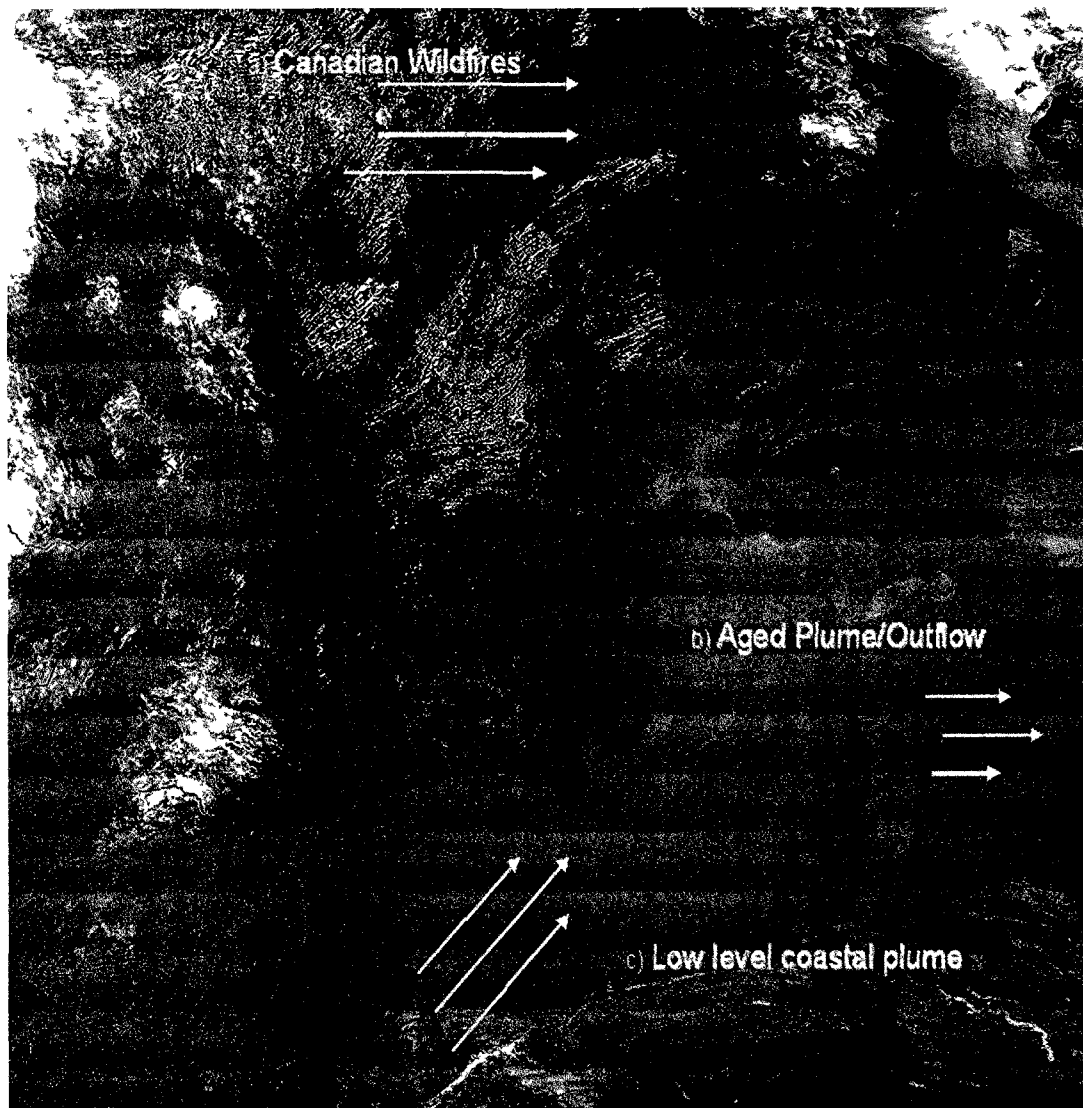
Figure 1.2. MODIS Satellite imagery of mixed pollution plumes over the North Atlantic and East Coast on July 20, 2004. Identifiable are a) wildfires from Alaska and Western Canada, b) aged emissions over the Western Atlantic, and c) recently vented pollutants from the NYC source region traveling at low altitude over coastal waters.

1.2 Region of Interest

To examine the influences of the lower marine atmosphere on GOM trace gas behavior and pollution plume transport/outflow, a suitable region of interest was established. Specifically, a domain was defined between 40°-48° N in latitude and 63°-74°

W in longitude and as shown in Figure 1.3a. This domain includes the two dominant source regions in or adjacent to the GOM: Boston, MA and New York City, NY. Also identified in the figure are Massachusetts Bay and Long Island Sound, the prominent over-water pathways for regional plume transport. In the inset of the map are the locations of the AIRMAP surface data stations used (Figure 1.3b), as described below.

1.3 Observational Data

The primary data used in this study was obtained during the International Consortium for Atmospheric Research on Transport and Transformation (ICARTT) field campaign in 2004. As described in Fesenfeld et al. 2006, ICARTT was an extensive field experiment that spanned the entire North Atlantic region, with the involvement of an unprecedented array of research aircraft, research vessels, mobile wind profilers, balloon platforms, as well as the extensive surface networks of chemical and meteorological observations. For this study, the primary airborne observations used were obtained onboard the National Oceanic and Atmospheric Administration (NOAA) WP-3D Orion and the National Aeronautics and Space Administration (NASA) DC-8 research aircraft. On land, surface observations from the AIRMAP regional air quality network were used exclusively. Over the coastal and open ocean regions of the GOM, a mixture of observations recorded onboard the NOAA research vessel R/V Ronald H. Brown and measurements obtained from the National Data Buoy Center stations maintained in the region were used. Further details on the observational data and methodology are presented in the relevant chapters which are introduced below.
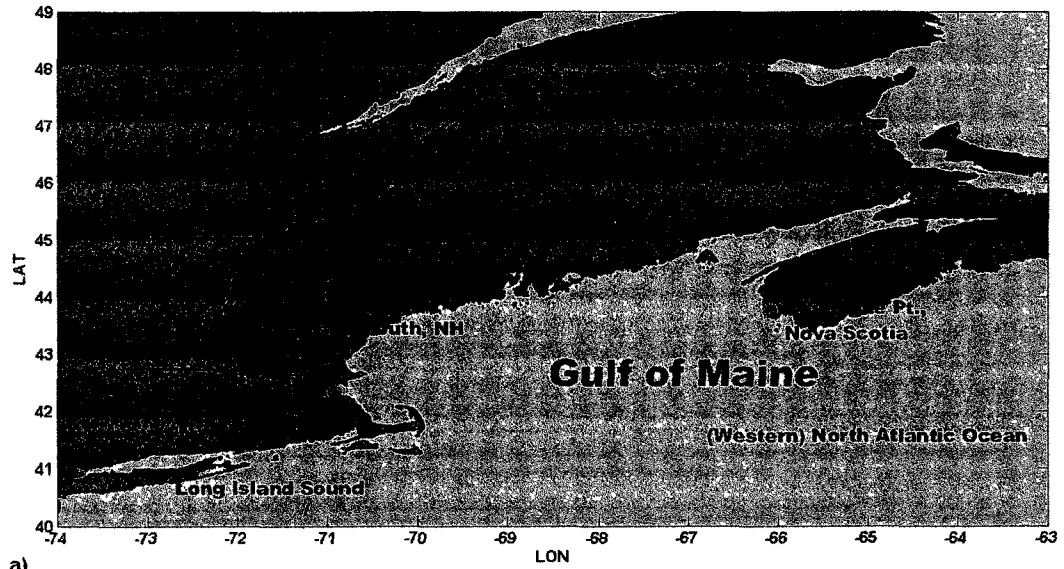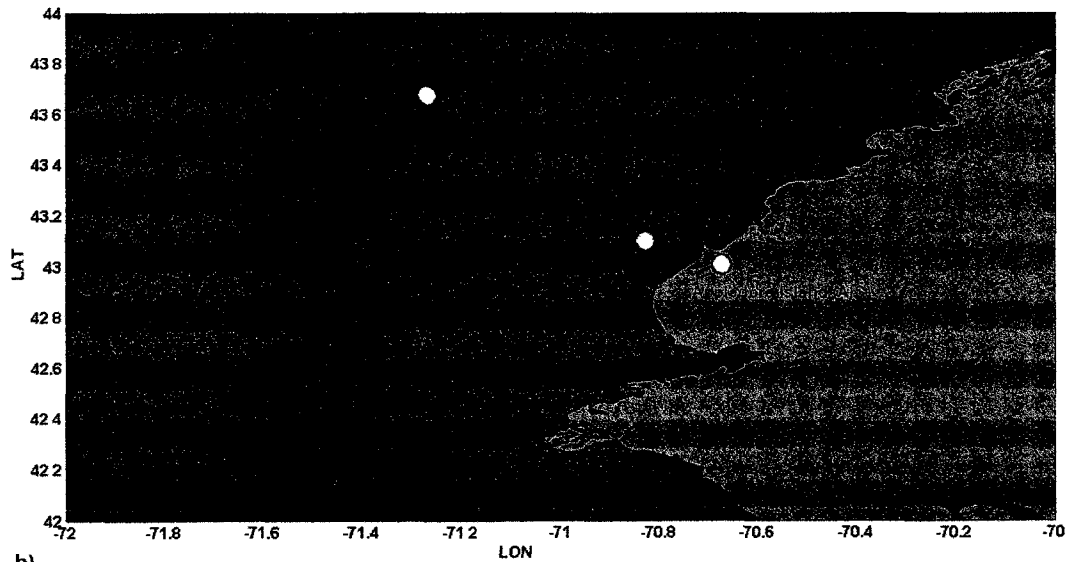
Figure 1.3. a) Maps of the Gulf of Maine and surrounding region, the domain of interest, and b) the AIRMAP air quality network.

1.4 Study Goals

With the use of the data described, the primary focus of this work has been to pursue an examination of coastal dynamical influences on trace gas observations and

6

transport in the GOM western North Atlantic. In this study, Chapter 2 advances a unique quasi-lagrangian analysis of a low levels plume through the GOM. Specifically, a recently ventilated plume is tracked from Long Island Sound to the northern GOM, and analyzed through multiple aircraft intercepts as it and the surrounding marine-atmospheric layers transform over a three day period. Chapter 3 builds on this, with an extended investigation of the influences of a stable internal boundary layer on plumes and coastal trace gas variability. A summary of the key points, conclusions, and plans for future work is presented in Chapter 4.

CHAPTER 2: TRANSPORT AND OUTFLOW TO THE NORTH ATLANTIC IN THE LOWER MARINE TROPOSPHERE DURING ICARTT 2004

Abstract

An analysis of pollution plumes emitted from sources in the Northeastern U.S. was based on observations from the International Consortium for Atmospheric Research on Transport and Transformation (ICARTT) 2004 field campaign. Particular attention was given to the relation of these plumes to coastal transport patterns in lower tropospheric layers throughout the Gulf of Maine (GOM) and their contribution to large-scale pollution outflow from the North American continent. Using measurements obtained during a series of flights of the NOAA WP-3D and the NASA DC-8, a unique quasi-lagrangian case study was conducted for a freshly emitted plume emanating from the New York City source region in late July, 2004. The initial development of this plume stemmed from the accumulation of boundary layer pollutants within a coastal residual layer where weak synoptic forcing triggered its advection by mean southwesterly flow. As the plume tracked into the GOM, analysis showed that the plume layer vertical structure evolved into an internal boundary layer form, with signatures of steep vertical gradients in temperature, moisture and wind speed often resulting in periodic turbulence. This structure remained well-defined during the plume study, allowing for the detachment of the plume layer from the surface and thus minimal deposition and plume-sea surface exchange. In contrast, lateral mixing with other low-level plumes was significant during its transit and facilitated in part by persistent shear driven turbulence

which further contributed to the high spatial variability in trace gas mixing ratios. The impact of the plume inland was assessed using observations from the AIRMAP air quality network. This impact was noticeably detected as a contribution to poor surface ozone conditions and significant elevations of other major pollutants to levels equaling the highest observed that summer. Further contributions to larger-scale outflow across the North Atlantic was also observed and analyzed.

1. Introduction

The composition and dynamics associated with pollution plumes released from coastal source regions is of eminent importance to regional air quality and larger scale continental outflow. Over the Northeastern coast of the U.S., this is especially true, where pollution plumes are regularly emitted from urban/industrial sources along the East Coast that directly impact downwind locations in coastal New England and Eastern Canada (Mao and Talbot, 2004a; Millet et al., 2006; Angevine et al., 2006; Mao et al., 2006; Chen et al., 2007). It has further been observed that frequently these plumes contribute to large scale pollution outflow, traveling 100s to 1000s of kilometers in stable lower tropospheric layers over the Atlantic Ocean, eventually adding to aggregated flows of pollutants that comprise North American continental outflow. Like the upper level forms of outflow (i.e. that facilitated by warm conveyor belts), these flows can measurably influence the composition of the marine atmosphere as well as surface conditions in western and central Europe (Stohl and Trickl, 1999; Stohl et al., 2001; Eckardt et al., 2004; Simmonds et al. 2004).

Low level outflow (LLO) is a form of continental outflow which is achieved within the lower tropospheric layers and occasionally the marine atmospheric boundary layer (MABL) itself. In previous studies, LLO has been identified as pollutant flow leaving the continent and traveling below 3 km in altitude (Daum et al, 1998; Owen et al, 2006). Such case of outflow can result from a variety of forcing mechanisms. Cooper et al (2002) identified the post-cold front air stream as one common mechanism of ventilation into shallow layers of the troposphere during the passage of weaker low pressure systems and full mid-latitude cyclones. Case studies of lower tropospheric

transport over the North Atlantic during the summer of 2003 by Owen et al. (2006) suggested a range of meteorological conditions may lead to the onset of LLO events. Employing Lagrangian model simulations in support of observations at PICO NARE, Owen et al. (2006) analyzed three cases of LLO in response to forcing of North American pollution into the lower free troposphere (0-2 km) by weak synoptic activity and the maintenance of shallow detached layers across the Atlantic.

Most similar instances of LLO begin as regional scale processes where pollutant laden continental air masses undergo significant transformations at the coastal boundary as they move into the marine atmosphere. These transformations are forced by abrupt land-sea differences in roughness lengths, vertical moisture and heat fluxes, as well as surface temperature gradients present along the coastline (Angevine et al 1997, 2002, 2006; Owen et al 2005; Millet et al., 2006). Numerous efforts have described such scenarios, including the recent study by Dacre et al. (2007) which connected shallow ventilation and boundary layer trace gas transport to local mesoscale processes such as the sea-breeze and regional coastal land-sea flow patterns. In such scenarios, pollutants are deposited into the shallow residual layers over cold North Atlantic waters. These residual layers often evolve into a stable internal boundary layer (SIBL) above the marine boundary layer and the cold North Atlantic waters (Garratt, 1990; Angevine et al, 2006). Importantly, this further implies that LLO and the shallow ventilation of boundary layer pollutants may then occur in the absence of strong, synoptic scale forcing events.

Recent efforts have shown that influence of LLO events on regional as well as intercontinental transport has been significant. In regional analyses, Chen et al. (2007) employed principal component analysis in determining that 58% of the variance of the

airmasses influencing northern New England was associated with emissions from nearby coastal source regions such as Boston and NYC. Over larger scales, Li et al. (2005) concluded from extensive model simulations that 30% of the North American CO exported in the summertime occurs below 3 km in altitude.

These findings provide motivation for the present study which builds upon previous efforts to better understand LLO and coastal circulation as transport pathways of the North American continental outflow, and the dynamics of the lower troposphere/MABL that facilitate it. The NOAA WP-3D flights in particular during the ICARTT campaign yielded invaluable observations of the composition and structure associated with low level pollution transport from the Eastern U.S. during the summer of 2004. Of these flights, three sequential flights between July 20th and July 22nd provided the unique opportunity to observe flow of a freshly emitted plume along the northeast coast, into the Gulf of Maine (GOM) and its eventual outflow into the western North Atlantic. Specific objectives of our study were to employ these observations in a quasi-Lagrangian manner to investigate the composition and dynamics of such regional plumes, influences of the local MABL on plume transport, and the contribution of such plumes to North American continental outflow.

2. Data

The primary trace gas observations in the coastal and marine atmosphere investigated here were obtained onboard the NOAA WP3-D Orion research aircraft (P-3). In its configuration for the ICARTT 2004 campaign (Fehsenfeld et al., 2006), carbon monoxide (CO) and sulfur dioxide (SO_2) were measured from sensors on the wing pod

with a fast-response, high-precision vacuum ultraviolet (VUV) resonance fluorescence technique. Ozone (O_3), nitric oxide (NO), and nitrogen dioxide (NO_2) were measured onboard by chemiluminescensce methods. Total reactive nitrogen (NOy) was determined using a catalytic reduction technique with the aid of an AU converter. In-situ volatile organic carbon compounds (VOC's) were sampled using a proton transfer reaction mass spectrometer with additional can samples measured using a gas chromatograph - mass spectrometer. Chemical ionization mass spectrometers were used in the observation of peroxycarboxylic nitric anhydrides (PANs), nitric acid (HNO_3), sulfuric acid (H_2SO_4), and the hydroxyl radical (OH). Corresponding observations of additional physical and chemical parameters taken onboard the NASA DC-8 were further used in the analyses made. This data was freely available at the NASA Earth Missions webpage: http://www.espo.nasa.gov/intex-na/.

Surface observations from the AIRMAP measurement network (http://airmap.unh.edu) were used in the assessment of the out-flowing plume impact on coastal, near-coastal, and inland regions of the GOM. One minute averages of CO, O_3, and NO_y from the AIRMAP observatories at Appledore Island (AIS), Thompson Farm (TFR), and Castle Springs (CSP) during the ICARTT campaign were the primary surface data sets. The period of May, 1st to September 1st, 2004 was used in the statistical description of seasonal surface conditions at each site.

Based on the aircraft observations of meteorological parameters, wind speed, wind direction, water mixing ratio, and potential temperature, further useful parameters were determined to gain insight into the stability and turbulent properties of the plume transport layers. Virtual potential temperature, θ_v, is the theoretical potential temperature

of dry air that would have the same density as moist air and was calculated by the relationship:

$$\theta_v = \theta(1 + 0.6r - r_l)$$

(2.1)

using potential temperature and water mixing ratio (r, water vapor mixing ratio and r_l, liquid water mixing ratio) measurements. The vertical gradient of the virtual potential temperature was calculated from vertical profiles made during the WP-3D flights to provide information in the stratification stability.

Using the θ_v profiles and observations of vertical shear in the horizontal wind vectors, the gradient Richardson number, R_i, was calculated using:

$$Ri = \frac{\frac{g}{\theta v}\frac{\partial \theta v}{\partial z}}{\left(\frac{\partial U}{\partial z}\right)^2 + \left(\frac{\partial V}{\partial z}\right)^2}$$

(2.2)

R_i is a nondimensional ratio that relates the buoyant production or consumption of turbulence to the shear production of turbulence within atmospheric layers. In this study, R_i was used to gauge dynamic stability and the formation of turbulence within a layer. A value of R_i =0.25 has been established as a critical value separating laminar from turbulent behavior in most geophysical flows. This is based on solutions to the Taylor–Goldstein form of the linearized Navier–Stokes equation quasi-2dimensional flows as described in Kundu (2004). Below the 0.25 value, shear driven Kelvin–Helmholtz instability is manifested forcing turbulent characteristics in the flow.

Observations of wind speed (instantaneous and 5 second averages) and wind direction were also employed to calculate the turbulent kinetic energy (TKE) within layers:

14

$$\frac{TKE}{m} = \bar{e} = 0.5\left(\overline{u'^2} + \overline{v'^2} + \overline{w'^2}\right) \qquad (2.3)$$

As shown, this is the mean kinetic energy per unit mass associated with eddies and turbulent motion within a given layer.

3. Results and Discussion

A total of sixteen research flights were conducted by the NOAA P3 aircraft between July 5th and August 14th 2004 in conjunction with the ICARTT campaign. Three of these flights were flown between July 20th and July 22nd (hereafter flights 7/20, 7/21, and 7/22 respectively) to provide a quasi-Lagrangian vantage point of a fresh plume (hereafter the 7/20 plume) emitted from the NYC source region as it transited through the GOM and into the Western North Atlantic.

3.1 Development of the plume

The 7/20 plume case study was characteristic of a low-flowing fresh plume, ventilated into shallow tropospheric layers by weak synoptic forcing. Regional lower tropospheric conditions captured by the National Center for Environmental Prediction (NCEP) analyses of surface pressure, and 10 m wind vectors during the Lagrangian experimental timeframe reflect a slow southwesterly flow off the east coast from Virginia to Newfoundland (Figure 1a). This flow was established primarily under the influences of the Bermuda High to the southeast of the source region and the Canadian low pressure

15
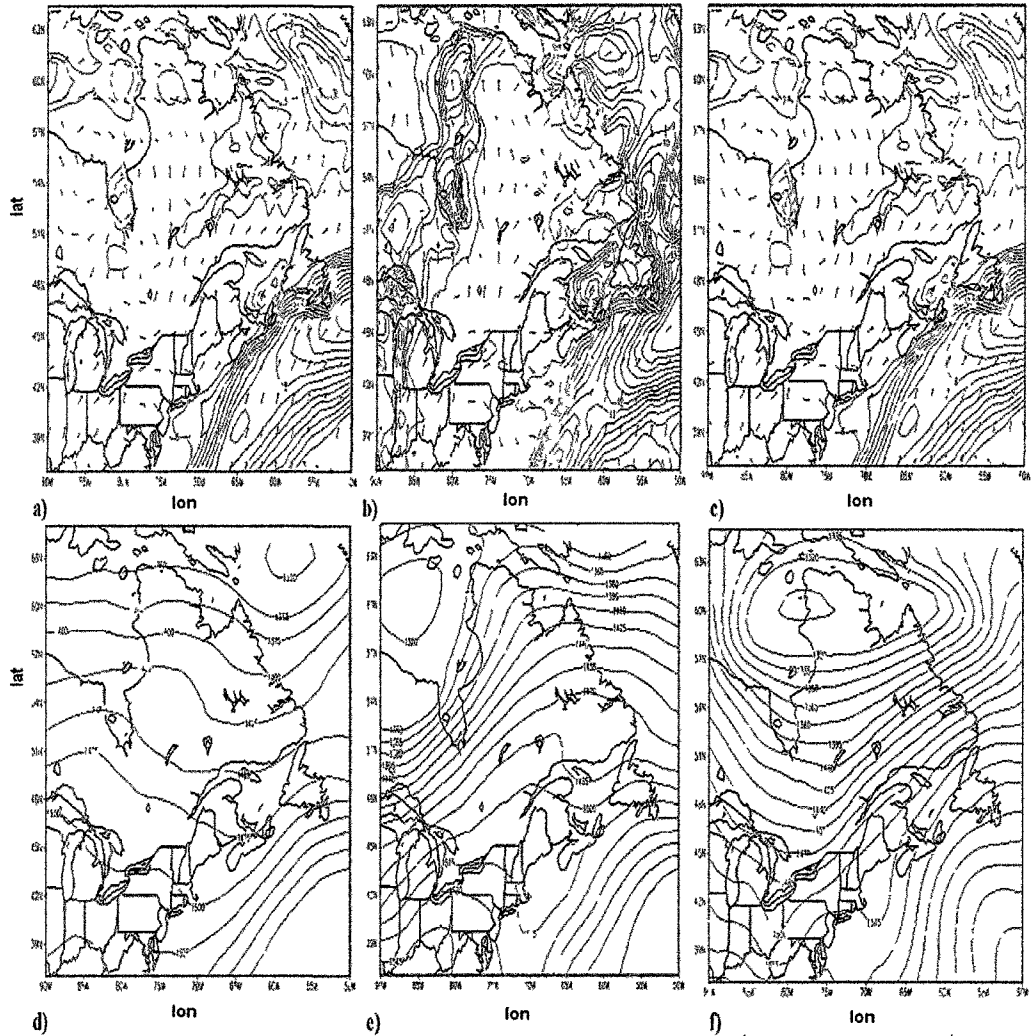
Figure 2.1. NCEP Reanalysis of mean sea level pressure and surface wind vectors for a) July 20th, b) July 21st and c) July 22nd during the 2004 ICARTT campaign. 850mb geopotential heights are shown for the same respective dates in d), e) and f).

system initially centered to the northwest along the northern edge of Hudson Bay. Upper level patterns similarly depicted the influence of these large-scale features within the region with the jet stream maintained northwest of the Great Lakes supplying a relative northeasterly flow aloft. The 'trigger' for the ventilation of the plume was the

16

development of a mild mesoscale low pressure trough between these larger synoptic features over the mid-Atlantic states developing near the surface as the Canadian Low translates progressively eastward during the 21st and 22nd (Figures 2.1 b, c).

3.2 Day 1: Initial Characterization of the Low-Level Plume

3.2.1 Chemical Composition near Long Island Sound

Initial encounters by the P-3 with the plume occurred on July 20th. Departing at 1400Z, this first mission in the three day experiment conducted an eight hour survey of the plume, making multiple crossings between Long Island Sound (LIS) and the southern GOM as depicted in Figure 2. During the flight, the physical and chemical signatures of the plume were distinct near the NYC source region and coastal atmosphere surrounding LIS. Above these waters and throughout the immediate Atlantic coastline, a series of vertical profiles between 1530Z and 1830Z observed the plume as a polluted airmass residing within a 1500m thick layer at a mean altitude of 1000m above the surface and flowing with a southwesterly trajectory.

Figure 3 shows the initial structure of the 7/20 plume as distinguished in the 1830Z vertical profile of its primary constituent species: CO, O_3, SO_2, and HNO_3. The vertical center of the plume was detected at a height of 1300 m, coinciding with a peak in the CO mixing ratio (170 ppbv) and an accompanying elevation in O_3 (76 ppbv). Further extremes in industrial/urban indicators were observed at this altitude, including
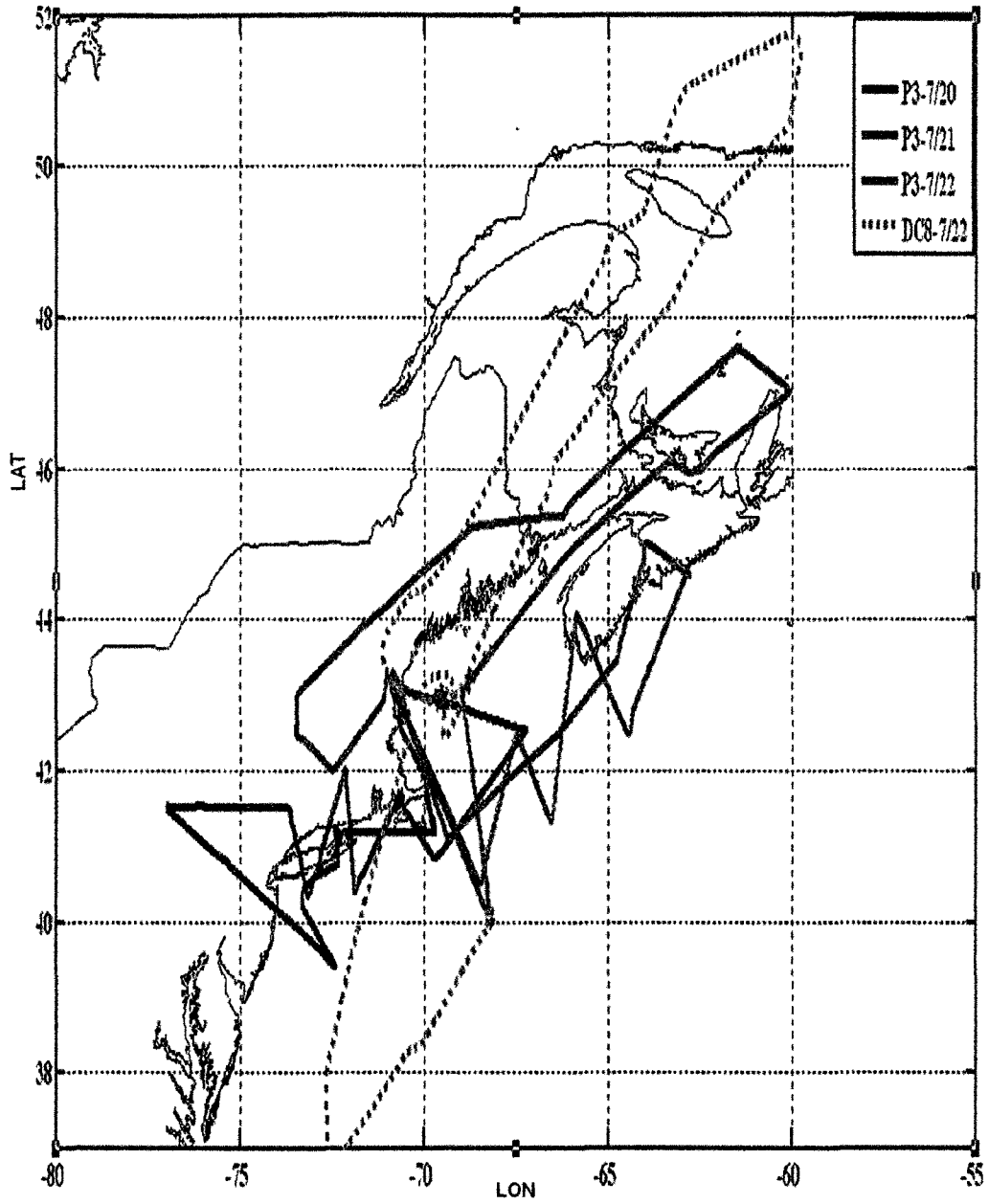
Figure 2.2. Flight tracks of the NOAA WP-3 and NASA DC-8 on 7/20, 7/21 and 7/ 22.

pronounced enhancements in toluene (798 pptv), methyl ethyl ketone (MEK) (1268 pptv), and benzene (268 pptv) (Table 1) which are characteristically emitted from heavy industry (solvent use) and automobile emissions. An elevation to 2.9 ppbv in SO_2 in the plume's vertical center was also observed and likely derived from regional power plant emissions.

Observations of enhanced mixing ratios of reactive nitrogen were similarly made in the plume's core over NYC, with NO_y measuring 3.0 ppbv and predominantly comprised of HNO_3 (2.8 ppbv). Following the method set forth in Kleinman et al. (2008) and more recently pursued in Slowik et al. (2011), the photochemical age of the plume was estimated in terms of these observations. Specifically, the NO_x-NO_y ratio was employed in the relation:

$$age \cong -\log([NOx]/[NOy]). \tag{2.4}$$

As detailed in the reference works, a value of 0 is indicative of fresh emissions while 1 represents photochemical aging of 1 day or more. For the 7/20 plume, mean mixing ratios of NO and NO_2 were 0.035 ppbv and 0.16 ppbv respectively in the plume core over NYC. Mean NO_x levels were then 0.195 ppbv establishing a mean NO_x /NO_y ratio of 0.0676 and a corresponding approximate photochemical age of 1-2 days. Two-day NOAA HYSPLIT Lagrangian back trajectories supported this conclusion, indicating that the plume followed a shallow recirculation over coastal and eastern New York, Pennsylvania, and New Jersey during the two days prior to the initial P3 intercept as shown in Figure 4.
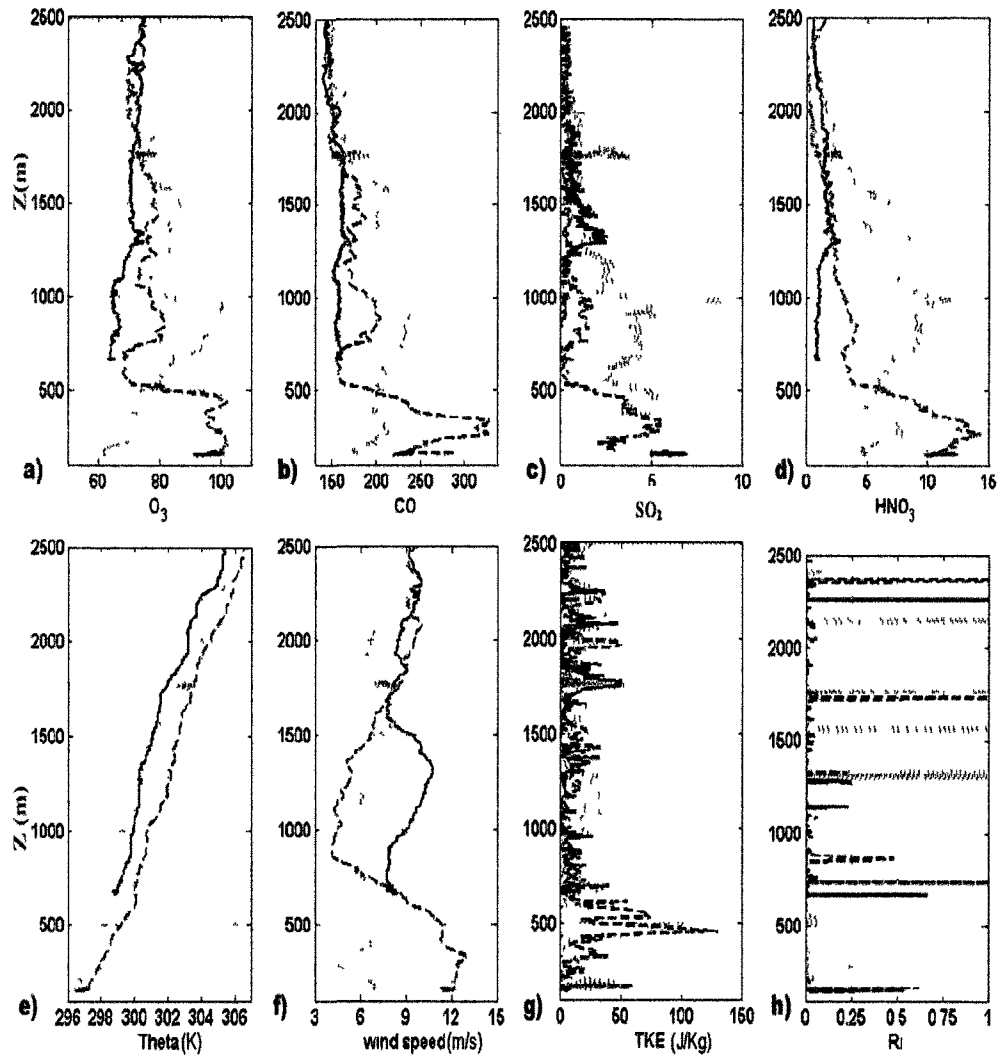
Figure 2.3. Vertical profiles of primary trace gas species and physical parameters observed near the NYC source region on 7/20. Shown are mixing ratios for a) O_3, b) CO, c) SO_2 and d) HNO_3 (all in ppbv) along with e) potential temperature f) horizontal wind speed, g) turbulent kinetic energy, and h) Richardson number. Black lines correspond to the observations directly over the NYC region at 1830Z; grey dotted lines designate the evolution observed 130km downwind of NYC at 1920Z; and dark grey dashed lines mark observations 250km downwind at 20Z.
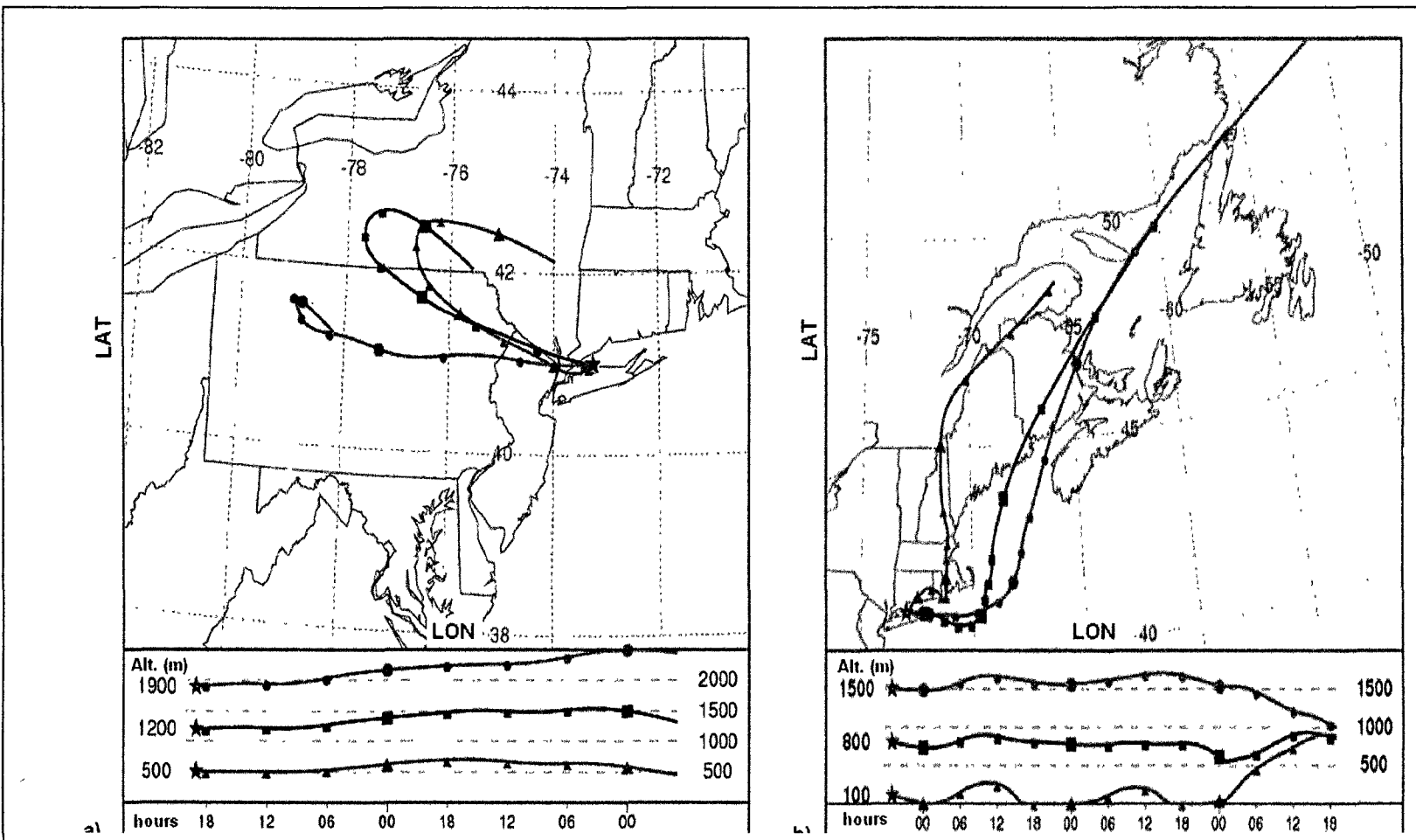
Figure 2.4. NOAA HYSPLIT lagrangian model simulations showing the probable a) back trajectories for two days prior to the initial encounter with the 7/20 plume by the WP-3D and b) forward trajectories for five days following the same encounter.

The relationships between the primary trace gas constituents in the plume were further examined to provide additional insight into its origins and relative background mixing ratios of the species in the lower troposphere over LIS. Considering CO as a general indicator of combustion, its correlation with O_3 was employed to gauge photochemical processing within polluted airmasses. Initial encounters with the plume on the 20th suggested that O_3 and CO were well correlated (correlation coefficient of 0.83) in close proximity to the NYC source region above LIS. As shown in Figure 5a, O_3/CO ratios within the plume profile near the source region displayed a strong linear relationship, with a regression slope of 0.21 and corresponding correlation coefficient (r^2) of 0.53. This slope is slightly less than the 0.26 values observed by Daum et al. (1996) in similar low flying plumes emanating from the northeastern US and tracked over the Atlantic during the 1993 North Atlantic Regional Experiment (NARE) a decade earlier. This finding maintain the trend of O_3/CO slopes being significantly less in plumes over the North Atlantic than over coastal and inland locations. Specific cases include Mao and Talbot (2004b) who observed mean summertime O_3/CO slopes of 0.37 using three years of data from AIRMAP surface sites and Chin et al. (1994), who determined a mean 0.3 slope to be typical within photochemically aged airmasses found in lower tropospheric layers above summertime North America.

The O_3/NO_y relationships derived from the same vertical profiles similarly exhibited correlation between the species. However, some variability resulted from probable depositional losses of NO_y species and possible mixing of aged and fresher emissions within the plume given its two day history. In the 1830Z intercepts, it was seen
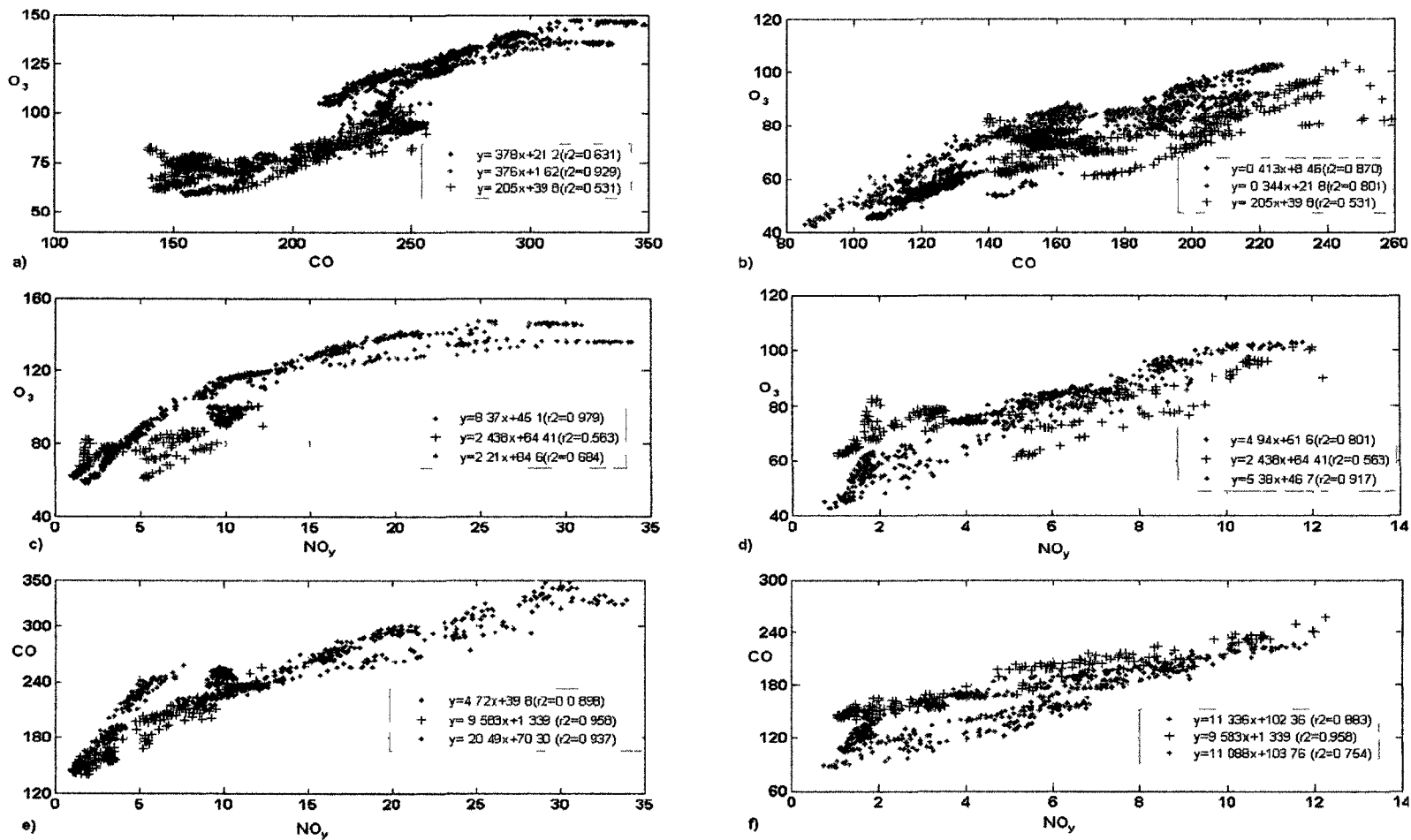
Figure 2.5. Selected trace gas relationships with the plume layer and parameters for corresponding linear fits. Shown are O_3/NO_y, O_3/NO_y and CO/NO_y for the coastal GOM P3 aircraft observations in a), c) and e) respectively and for the open ocean observations in b), d) and f). Black marks designate observations within the plume over the NYC source region on 7/20, blue markers designate observations over the GOM on 7/21 and green markers designate observations over the GOM on 7/22 with all values being in ppbv.

that a weaker linear relationship (r^2= 0.63) was observed between O_3 and NO_y, (Figures 5c, d) suggesting that a mixture of airmasses may have been intercepted during initial plume encounters. At higher NO_y levels (>8 ppbv), the correlation is clearly higher (0.68), and reflective of recent emissions, while at lower mixing ratios of NO_y (<5 ppbv), the correlation was less (0.49), more suggestive of photochemically aged airmasses and loss of NO_y through deposition. The CO/NO_y relationship exhibited clear linearity, with a fitted slope of 9.583 (r^2 =0.95) as seen in figure 5e. Such close correspondence between CO and NOy is indicative of a common combustion source such as automobiles (Daum et al, 1996).

Analysis of whole air samples (WAS's) obtained during the near-source region vertical profiles provided insight into 74 additional chemical species within the 7/20 plume (Table 2.1). Halocarbons in these samples were of particular interest, since they are generally found well mixed in the troposphere except in close proximity to source regions (Blake et al, 2004). Many halocarbons also have relatively long lifetimes, with their primary removal mechanism being their reaction with OH (Thomson et al., 2005). Halocarbon species function well as urban industrial tracers and as seen in this analysis, are a means of tracking the 7/20 polluted airmass. Specific halocarbons observed in the 7/20 plume included the industrial solvent dichloroethane ($C_2H_4Cl_2$), observed at 5.37 pptv within the plume layer, relative to a background mean of 31 pptv observed throughout the remaining flight. Similar enhancements in the level of the dry cleaning agent tetrachloroethylene (C_2Cl_4) were observed at 188 pptv near the source region. These levels can be compared to a background of 22 pptv determined in other segments

of the flight. The heavily used industrial rubber/plastic chloromethane (CH_3Cl) also had an enhanced mixing ratio of 531 pptv. Other non-halocarbon anthropogenic indicators were also present in the NYC WAS's, including the refining byproducts ethane (~ 2840 pptv) and ethene (~936 pptv), along with industrial fuel tracers propane (~1650 pptv), and acetylene/ethyne (~1063 pptv).

Correlations between the anthropogenic tracers in the plume WASs and CO were determined as shown in Table 1. At the 95% confidence level, the correlation coefficients calculated between the two of the most abundant anthropogenic halocarbons within the plume (CH_2Cl_2, $C2Cl_4$) and CO were above 0.95. Within the same confidence interval, correlation coefficients between tracers ethane, ethyne, benzene, and propane and CO also exceeded 0.95, further reflecting the anthropogenic origin of the plume and the close proximity to the source region.

Mixing ratios of non-anthropogenic indicators near the source region in the WASs also supplied insight in terms of plume history and structure. Isoprene, an indicator of air mass exchange with continental vegetation was observed at 800 pptv while dimethyl sulfide (DMS), an indicator of contact with marine surfaces, was detected at a mean of only 12 pptv within the plume. These observations suggest that during the previous days prior to the aircraft intercept, the plume air mass likely experienced some level of exchange with the land surfaces it passed over while only having limited contact or exchange with the sea surface during the same period. This detachment from the ocean surface was more apparent in the vertical profiles of the physical parameters as discussed below.

WAS Sample Species	720 Correlations	720 maxes	720 means	721 Correlations	721 maxes	721 means	722 Correlations	722 maxes	722 means
CFC_11	0.964	289 700	262.927	0.769	270 700	260.800	0.685	58271 000	57070.000
CFC_12	0.936	581.900	555 109	0.856	557.800	550.280	0.837	58278 000	57078 000
CFC_113	0.929	83.300	81 136	0.236	82 000	81.300	0.143	259.200	254.230
CFC_114	0.564	15 170	14 747	0.219	14.690	14.587	0.099	549 800	544 670
CFC_115	0.637	7 360	6 857	0.432	7.290	6 950	0.395	80.400	79 917
HFC_134a	0.972	227 400	95 018	0.916	105.500	76 917	0.442	14 630	14 488
HCFC_21	0.966	1 000	0 654	0.802	0.880	0 685	0.395	6.930	6 608
HCFC_22	0.924	756 600	313 627	0.733	324.300	259 330	0.661	63.300	52.317
HCFC_123	0.963	1 000	0 440	0.431	0 650	0 478	0.397	0 660	0 533
HCFC_124	0.560	11 100	3 452	0.652	4 040	2.560	0.686	224.800	201.600
HCFC_141b	0.880	49 440	26 653	0.927	27.350	24 015	0.769	0.370	0.300
HCFC_142b	0.965	41.560	26 164	0.962	30 670	24 983	0.528	1.950	1.573
CH2Cl2	0.893	264.100	82 773	0.926	63.600	43.850	0.802	23 770	21 478
CHCl3	0.979	28 780	17.297	0.916	22.310	16 432	0 798	22.680	20 525
X1_2_dichloroethane	0.859	5.370	4 762	0.731	4 440	4 283	0.354	39 700	30 483
CH3CCL3	0.976	28.600	25 055	0.952	25 700	24 483	0.773	16 010	12 640
CCl4	0.550	98 000	96 091	0.167	98 000	96.333	0.162	4 900	4 398
C2Cl4	0.950	188.000	49.360	0.962	40.200	18 047	0.762	25 000	24 100
C2HCl3	0.859	28.000	8 945	0.953	5 800	3.022	0 697	96 000	95 667
Halon_1301	0.666	3.180	2 804	0.529	2.880	2 653	0.440	12.900	8.002
Halon_1211	0.953	6.020	4.744	0.907	4.850	4.510	0.704	1 400	0.853
Halon_2402	0.571	0 490	0 470	0.598	0 490	0 473	0.616	2.790	2.695
CH3Cl	0.447	531.000	516.000	0 105	537.000	521 170	0.203	4.560	4.358
CH3Br	0.613	10 600	9 375	0 193	11 400	10.050	0.319	0 470	0 450
CH3I	0.582	0 760	0 514	0.501	1.640	0 990	0.538	535 000	512.500
n_C3H7Br	0.411	32.800	798 764	0 982	5.810	3 003	0.810	19.200	9 420
CH2Br2	0.871	0 830	0 734	0.297	1 090	0.855	0.390	0 650	0.390
CHClBr2	0.948	0.320	0 170	0.664	0.360	0.222	0.518	1 800	1 310
CHBr3	0.856	1 160	0 740	0.306	2.910	1.562	0.197	0 720	0 667
OCS	0 146	455.000	426.273	0.848	473 000	443.330	0.310	0 140	0 107
DMS	0.410	15.510	803.595	0.434	0.390	0.240	0.478	0.960	0 480
MeONO2	0.995	5 470	3 526	0.434	0.390	0.240	0.478	0.960	0 480
EthONO2	0.919	6.560	4.276	0 868	7 480	5.205	0 715	1.310	0 635
i_C3ONO2	0.889	17 900	11 115	0.857	23.540	15.373	0.716	3.260	2 692
n_C3ONO2	0.950	2.500	1 414	0 853	2.780	1 795	0.728	4 720	3 417
X2_BuONO2	0.953	14.900	8.328	0.890	21.940	12 178	0.658	12.530	8.297
X3Me2BuONO2	0.966	4 570	2.350	0.940	5 830	2 688	0.726	1.340	0 938
X3_C5ONO2	0.930	5 610	2.926	0.912	7.580	3 968	0.778	8.320	5 563
X2_C5ONO2	0.956	7 820	3 886	0.923	10 020	4 848	0.771	1 750	0 928
ETHANE	0 960	2840 000	1693.273	0.501	2423 000	1591.200	0.587	2.240	1 533
ETHYNE	0.986	1062.400	472.036	0 954	493.900	313.680	0.824	2.350	1.568
ETHENE	0.512	936.000	599 000	0.708	140.000	53.333	0.585	1917.000	1466.800
PROPANE_FID	0 640	1642.000	252.364	0 884	1074 000	628.000	0.770	243.500	182.550
PROPENE	0.519	144 000	1774.000	0.799	11 000	7.667	0.624	20.000	14 167
PROPANE_MSD	0.956	1694.000	721 000	0.892	1029.000	620 670	0.774	383 000	272.830
I_BUTANE	0.969	519.500	162.218	0.851	193 100	96 700	0.455	13 000	7 167
N_BUTANE	0.974	670.500	225 755	0.964	255.100	122 180	0.781	374 000	269 170
I_PENTANE	0 985	811.200	279.909	0 968	182 100	88 850	0.830	43.200	24.550
N_PENTANE	0.980	338.300	111 945	0.965	87 000	43 150	0.827	48.300	33.900
ISOPRENE	0 173	800.800	218.555	0.915	0.800	0 467	0.185	37 700	18.117
BENZENE	0.980	268.200	108.745	0.905	111 000	69.617	0.823	17.200	9.517
TOLUENE	0.964	797.800	230.209	0.781	120 400	43 600	0.756	1 700	0.583
Ethyl_benzene	0.962	115 620	31.395	0.765	16.280	5.725	0 733	54 300	41 700
m_p_xylene	0.942	210 100	50.275	0.555	10 120	3.085	0.470	8.000	3 650
o_xylene	0.956	90.300	23 539	0.630	7 140	2.300	0.598	1 170	0 510
iso_propyl_benzene	0.957	9.260	2.554	0 806	2 030	0 802	0 712	0 790	0.343
X2_ethyl_toluene	0.930	34 190	8 078	0.589	2.150	0 808	0.581	0 700	0.368
X3_ethyl_toluene	0.923	59 820	13.509	0.519	2.220	0 808	0.429	0.390	0.258
X4_ethyl_toluene	0.931	35.280	8 193	0.559	1.930	0 643	0.580	0 660	0.322
1_3_5_trimethyl_benze	0.834	6.200	1 433	0.175	0.370	0.273	0.226	0.820	0.393
1_2_4_trimethyl_benze	0 910	44 990	10.253	0.498	1 440	1 013	0 140	0 420	0.207
1_2_3_trimethyl_benze	0.904	11 690	2 963	0.563	0.580	0 477	0.139	0.320	0 180
a_pinene	0 336	6 000	1.836	0.349	0.500	0.267	0 437	1.320	0.618
b_pinene	0 318	4.200	1 736	0.488	1.900	0 617	0.317	1 150	0 435
d_limonene	0 164	3.700	0 000	0.308	0 400	0 117	0.561	0 800	0 483
MTBE	0.878	295.700	60 109	0 666	125.500	44 533	0.639	0 600	0.383
Methacrolein	0.500	562.000	227.636	0.568	21 000	12.167	0.115	0.300	0.000
ETHYLETHYL_KETON	0 404	1268.000	677 545	0.627	75.000	31.333	0.364	10.900	4 433
X2_BUTANONE	0.895	980.000	445.545	0 885	571 000	406 670	0 706	23.000	12 333
X3_mefuran	0.575	41.500	12.245	0.277	9 100	5 467	0.532	51 000	26.500
CH4	0.961	1950 000	1856.818	0.807	1904.000	1858.500	0 460	287 000	200.500

Table 2.1. Analysis of Whole Air Samples taken within the plume layer over NYC on 7/20 as well as over the GOM on 7/21 and 7/22. Included are maximum and mean values for each species and correlations with CO calculated to the 95% confidence level in each case.

3.2.2 Physical Structure of the Plume Layer

The noticeable detachment of the 7/20 plume from adjacent vertical layers was a key aspect in its behavior as well as its evolution as a low level flow. Model back trajectories (Figure 2.4a) and synoptic charts support the hypothesis that the detachment and ventilation of the 7/20 plume was linked to the entrainment of continental boundary layer pollutants into a coastal residual layer formed in the lower troposphere rather than through the forcing of a single weather event. In this, the residual layer served as a shallow reservoir for continental pollutants and facilitated their outflow above the marine boundary layer in a detached plume-like fashion over LIS on 7/20. Similar observations of residual layer influences have been established in previous studies, particularly near land-sea transition regions, where buoyancy driven flows such as the land/sea breeze contribute to their development in the coastal atmosphere (Hsu, 1988). Over LIS, residual layers have frequently been found in summer months, when land-sea temperature contrasts are larger (Tardiff, 2005) and observed as reservoirs for boundary layer trace gas pollutants during air quality episodes along the East Coast (Zhang et al., 1998). In the study conducted here, data further suggested that the residual layer facilitated the long-range transport achieved by the plume through its advection into the lower troposphere and over the marine boundary layer, thus detaching it from surface interactions in a similar fashion to that described by Dacre et al (2007) and Foeschetto et al. (2001).

Directly above the source region, the physical state of the atmosphere surrounding the plume was characterized by well-stratified structure with stability evidenced by the profiles of θ (Figure 2.3e). The plume containing residual layer itself was distinguished by a jet-like increase in wind speed centered about a vertical peak of the plume (1300m),

27

with a maximum of 10.9 m s^{-1}. This enhanced wind speed was observed in conjunction with a ~30° shift in wind direction and a 20% increase in the water vapor mixing ratio compared to the layers surrounding the plume. The mean dew point temperature of the layer reached 19.3°C. Despite this near saturation of the plume layer, shear produced by the sharp vertical gradient in wind speed and direction appeared to also give rise to clear instances of periodic turbulence within it.

A value of 0.25 is considered to be the critical point for the R_i separating turbulent and non-turbulent regimes in the atmosphere (Garratt, 1990; Stull, 2008). Conditions favoring turbulence in the plume layers were observed in the near source region profiles, as indicated by values of R_i between 0.16 and 0.30 (Figure 2.3h). Coupled with this, an increase in vertical velocities was observed, ranging from 0.3-0.5 ms^{-1} (not shown). The enhanced vertical motion was also observed with in the plume layer, which coupled with the vertical gradient in the horizontal wind speed, contributed to significant increases in TKE at the upper and lower bounds of the plume layer (1700m and 980m respectively) (Figure 2.3g). These observations are further consistent with the diagnosis of mechanically driven turbulence in the layer, often taking the form of overturning motions associated with Kelvin-Helmholtz instability and leading to the development of small sub-grid scale eddies. The presence of this turbulence is inherent residual layers, and has been seen to influence air quality, via the down-mixing of pollutants during the growth of the mixing layer in the morning (Neu et al., 1994) while Mahrt et al (1999) suggested that transport within the residual layer is ensured by similar sporadic bursts of turbulence.

Additional aircraft intercepts on 7/20 captured the downwind transformation of the plume from an airmass residing in a residual layer to a shallow defined flow en route to the GOM. Induced through the influences of the intense wind shear observed in the lower marine troposphere, radiative cooling by the underlying sea surface, and the onset of the 7/20-7/21 nocturnal transition, initial stages of this transformation were observed at 1920Z, 130 km downwind of the NYC profile. Subsidence of the plume's vertical center down to 980m was evident in the profiles of O_3,CO, SO_2, and HNO_3 (Figures 2.3a-d, dotted lines). While horizontal wind speeds were reduced from their NYC magnitudes, periodic elevations in TKE were recorded in the plume profile and corresponding drops in the R_i values (Figures 2.3e-h, dotted lines) marked episodes of shear driven turbulence as seen earlier. Continued evolution was observed 300 km downwind as seen in profiles of trace gases and physical parameters observed at 20Z (Figures 2.3a-h, dashed lines). Between Narragansett Bay and Buzzards Bay, the aircraft observed the 7/20 plume as a distinct low level flow, detached from the surface layer and moving steadily out of the southwest. In this new configuration, the plume exhibited a 500m thickness, as distinguished in the trace gas profiles. The vertical center could be seen at 250-300m above the sea surface, where peaks of O_3, CO, SO_2, and HNO_3 reached 103 ppbv, 337 ppbv, 6 ppbv, and 14 ppbv respectively. A further distinguishable characteristic was a marked increase in horizontal wind speed, with maximum amplitudes reaching 12-13 m/s. Resulting horizontal shear contributed greatly to increased TKE (130 J/kg) as well as the persisting low R_i values (0-0.3) within the layer, strongly suggesting the continued presence of turbulent motion during the plume's transit.

3.3 Low-Level Plume Transit and Evolution on 7/21 and 7/22

Forward trajectories computed by the HYSPLIT model are shown in Figure 2.4b, projected a southwesterly track for the 7/20 plume over the 48 hours following the initial encounters by the P-3. This path was confirmed by Mao et al. (2006) through the analysis of SMART balloon observations which tracked the 7/20 plume from the source region to Newfoundland. Further verification of this trajectory was also achieved by multiple intercepts by the P-3 and DC-8 aircraft on 7/21 and 7/22, which additionally provided observations for the assessment of the plumes transformation. As discussed further below, clear differences in the plume's characteristics and its transformation were observed over the coastal as well as the "open ocean" waters of the GOM region.

3.3.1. (7/21~Day 2)

The NYC plume was readily identifiable during the flights on 7/21 through the analysis of the WASs obtained in the lower marine troposphere. As seen in Table 1, the signature of a high correlation between anthropogenic halocarbons and CO observed near the NYC source region was retained in the samples taken within the plume layer over the GOM on 7/21 and 7/22. The CH_2Cl_2-CO and C_2Cl_4-CO, and C_2HCl_3-CO correlations remained nearly unchanged on 7/21, each exceeding 0.9 at the 95% confidence level and facilitated tracking the plume while over the GOM region. Additional correlations determined between ethyne, propane, butane, benzene were similarly high, within a range of 0.8 to 0.9 with the same confidence interval. Yet, while continued to evolve significantly during the preceding 24 hours of its continued transit, with distinct

30
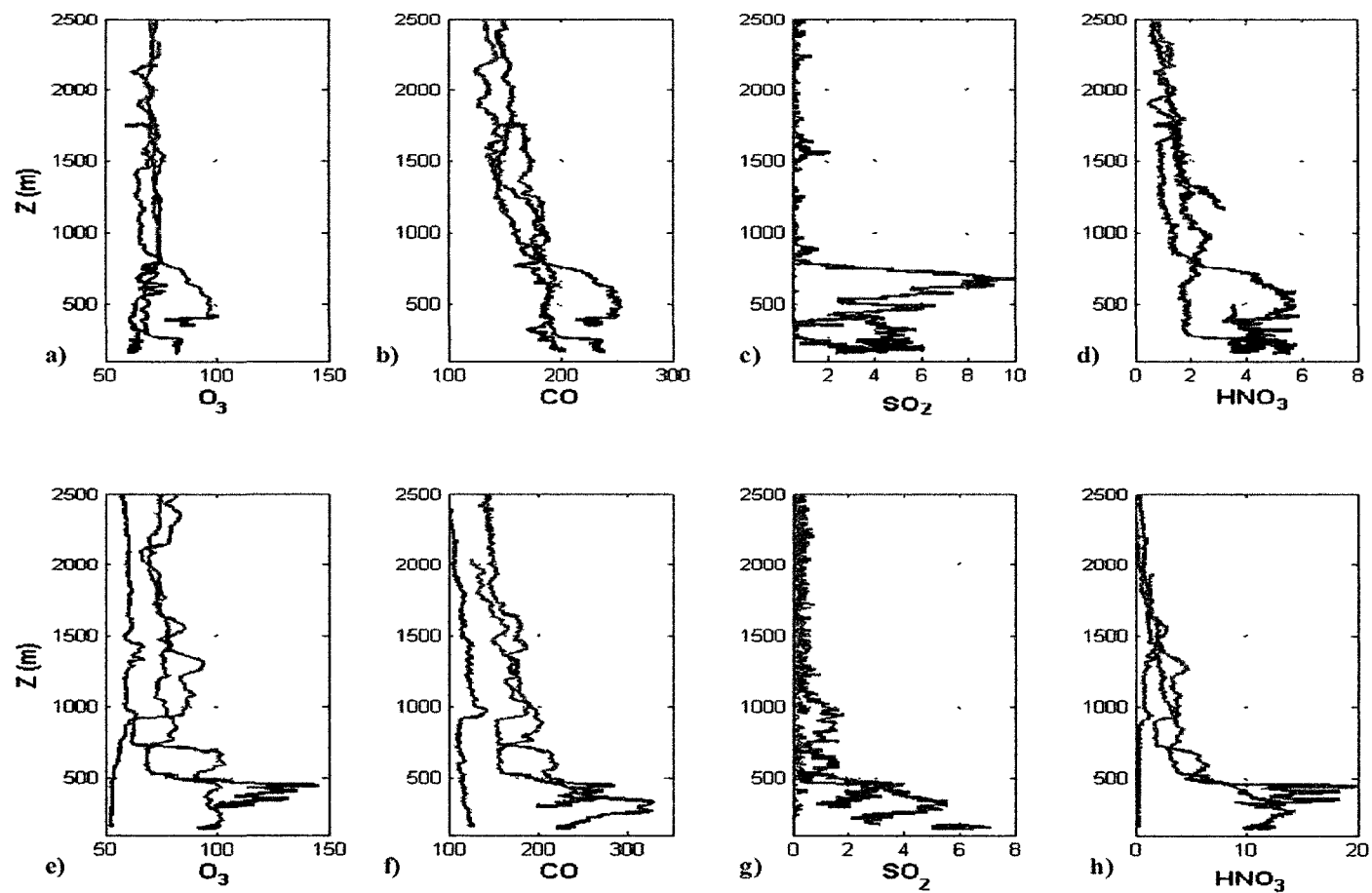
Figure 2.6. Aircraft profiles over the coastal GOM of a) O_3, b) CO, c) SO_2 and d) HNO_3. Corresponding observations of the same trace gas species over the western Atlantic/ eastern GOM are shown in e) -h). Blue lines represent observations on 7/20, red 7/21 and green 7/22 with all trace gas observations made in ppbv.
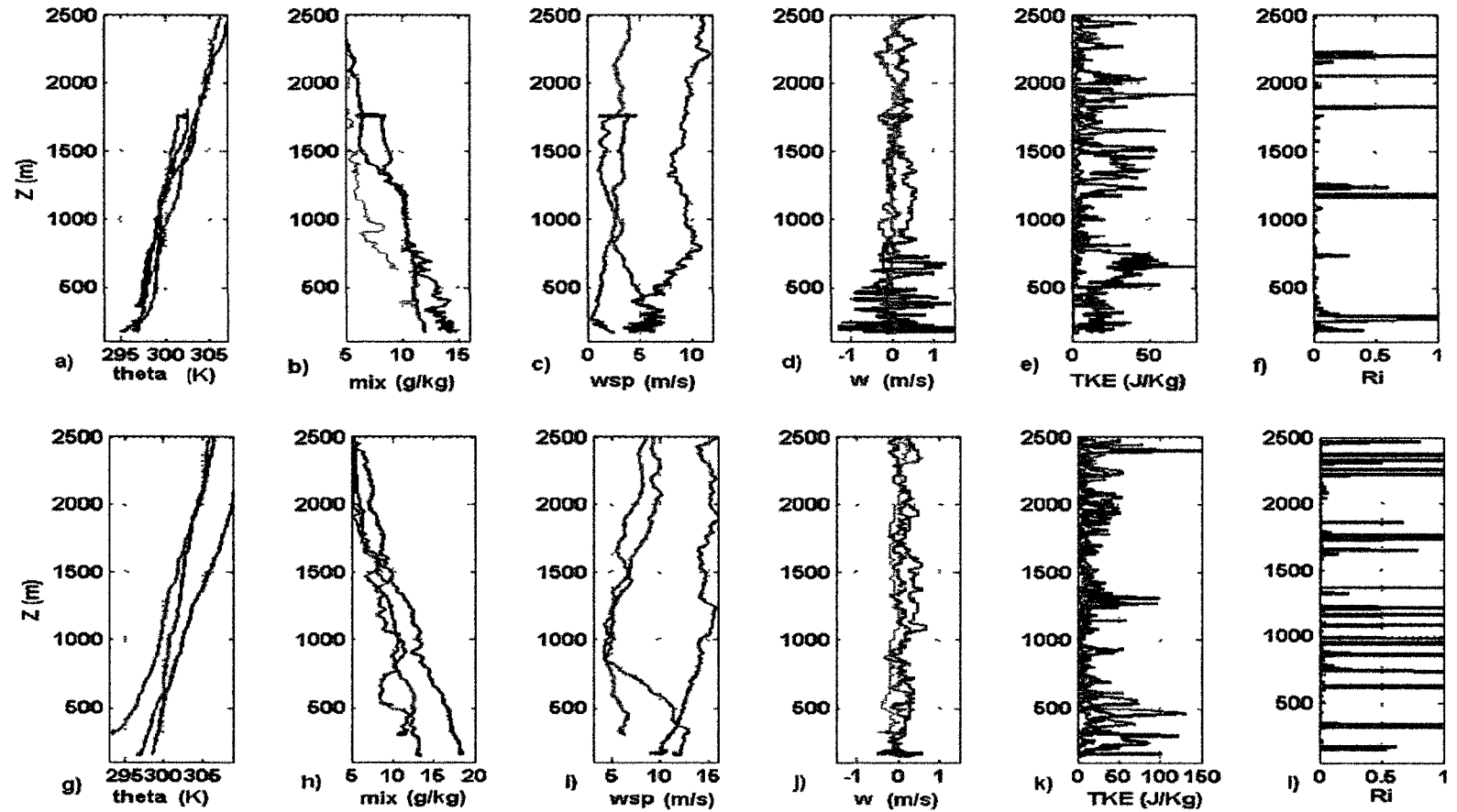
Figure 2.7. Aircraft profiles over the coastal GOM of a) potential temperature, b) water vapor mixing ratio c) horizontal wind speed d) vertical wind speed, e) turbulent kinetic energy, and f) Richardson number values. Corresponding observations of the same parameters over the western Atlantic/ eastern GOM are shown in g)-l). Blue lines represent observations on 7/20, red 7/21 and green 7/22.

differences in its characteristics over the coastal GOM versus the open North Atlantic.

Despite coalescing to one-quarter its near-source region thickness, large enhancements in the primary species still distinguished the plume layer over the GOM, where CO levels peaked in the coastal region at 246 ppbv, O_3 at 83 ppbv, SO_2 at 4.2 ppbv, HNO_3 at 5.8 ppbv , and benzene at 109 pptv (Figures 2.6a-d). A subsequent profile made 5 hours later to the northeast revealed the full lateral expanse of the plume as well as significant differences in its characteristics farther out to sea. As seen in Figures 2.6e-h, peak mixing ratios in the primary species over the open North Atlantic were similar to those observed nearer the coast, as CO reached 337 ppbv, O_3 103 ppbv, SO_2 7.2 ppbv, and HNO_3 12.9 ppbv. This difference appeared to be linked to reduced cooling (i.e. slightly warmer temperatures) of the plume layer further out to sea as well as the presence of more vigorous turbulent motion indicated by the larger amplitudes (roughly 2x) of TKE (Figures 2.7k).

Turbulent characteristics remained apparent throughout the majority of the vertical profiles over the GOM with R_t values persisting well below the 0.25 (Figure 2.7f and l) indicative of instances of dynamic instability. Spikes in TKE (Figure 2.7e) marked the upper and lower limits of the plume layer in much the same way that was observed near the source region; However, with the subsidence of the plume to a near surface altitude, the plume layer more closely resembled a coastal internal boundary layer (IBL) over the GOM than the residual layer encountered over NYC.

Internal boundary layers are frequently generated in the lower atmosphere and arise primarily from discontinuities in surface properties. In the case of the marine atmosphere, coastal IBL's result from air masses advected across the coastline, where

large differences in surface roughness and surface buoyancy (heat and moisture) fluxes are present on either side. In the case of the NYC plume, warm continental air trapped above the convective boundary layer in a residual layer was eventually advected into the lower marine troposphere. A resulting IBL formed based on significant differences in airmass between the plume and its new marine environment. This scenario was recently addressed by Dacre et al. (2007) while coastal IBL transport has been identified as a key aspect of regional transport particularly over the GOM in during a number of previous summer campaigns (Angevine et al., 1996; Smedman et al., 1997; Gong et al., 2000; Angevine et al., 2006).

A unique quality of this study was the Lagrangian observation of the plume with respect to the development of an IBL structure and the resulting impacts on trace gas processing and transport. In terms of physical characteristics, horizontal transects made by the P3 on 7/21 and 7/22 observed that many properties of the plume layer/IBL were remarkably constant over extensive distances across the GOM. As shown in Figures 2.8a-b, wind speed and potential temperature each exhibited smooth gradients within the plume layer, during a 160 km transect made over the southeastern GOM. A second 160 km transect performed to the northeast along the GOM-open North Atlantic transition region provided observations that similar structure persisted further out to sea. In each case, winds within the IBL/plume layer were consistently southwesterly, ranging from 2 to 5 m s^{-1}. Temperatures of the layer were similar as well, with a mean of 297.2 K, while the water vapor mixing ratio ranged from 10 to 14 g/kg.

In contrast, trace gas observations made during the same transects exhibited high
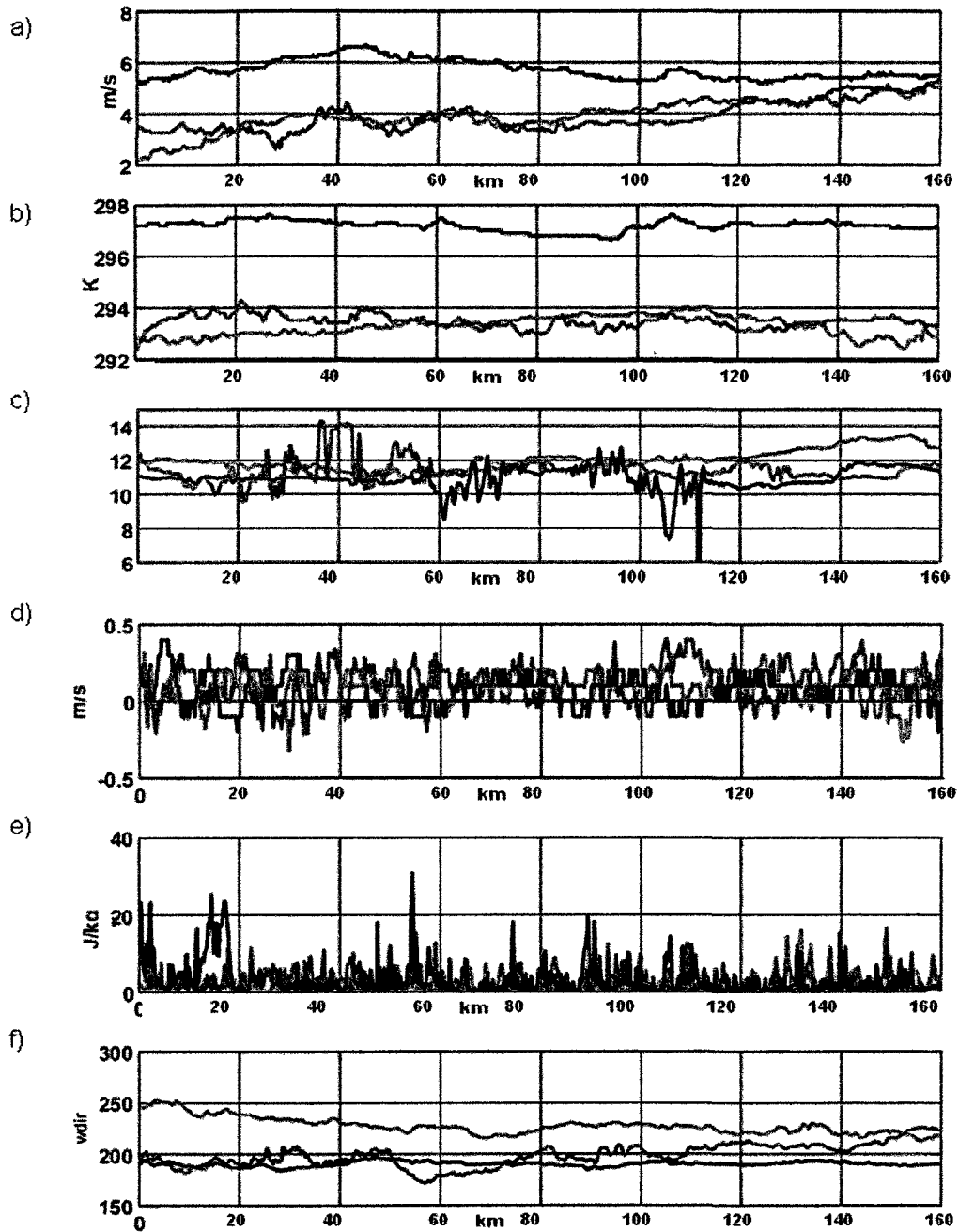
Figure 2.8. Physical characteristics of the NYC plume layer observed during transects by the P-3 on 7/21 and 7/22 over the GOM. Shown are a) horizontal wind speed b) potential temperature c) water vapor mixing ratio, d) vertical wind speed e) turbulent kinetic energy and f) wind direction. Cyan lines designate observations from the coastal GOM transect on 7/21, magenta lines the oceanic GOM transect on 7/21, and black lines the central GOM transect on 7/22.

35
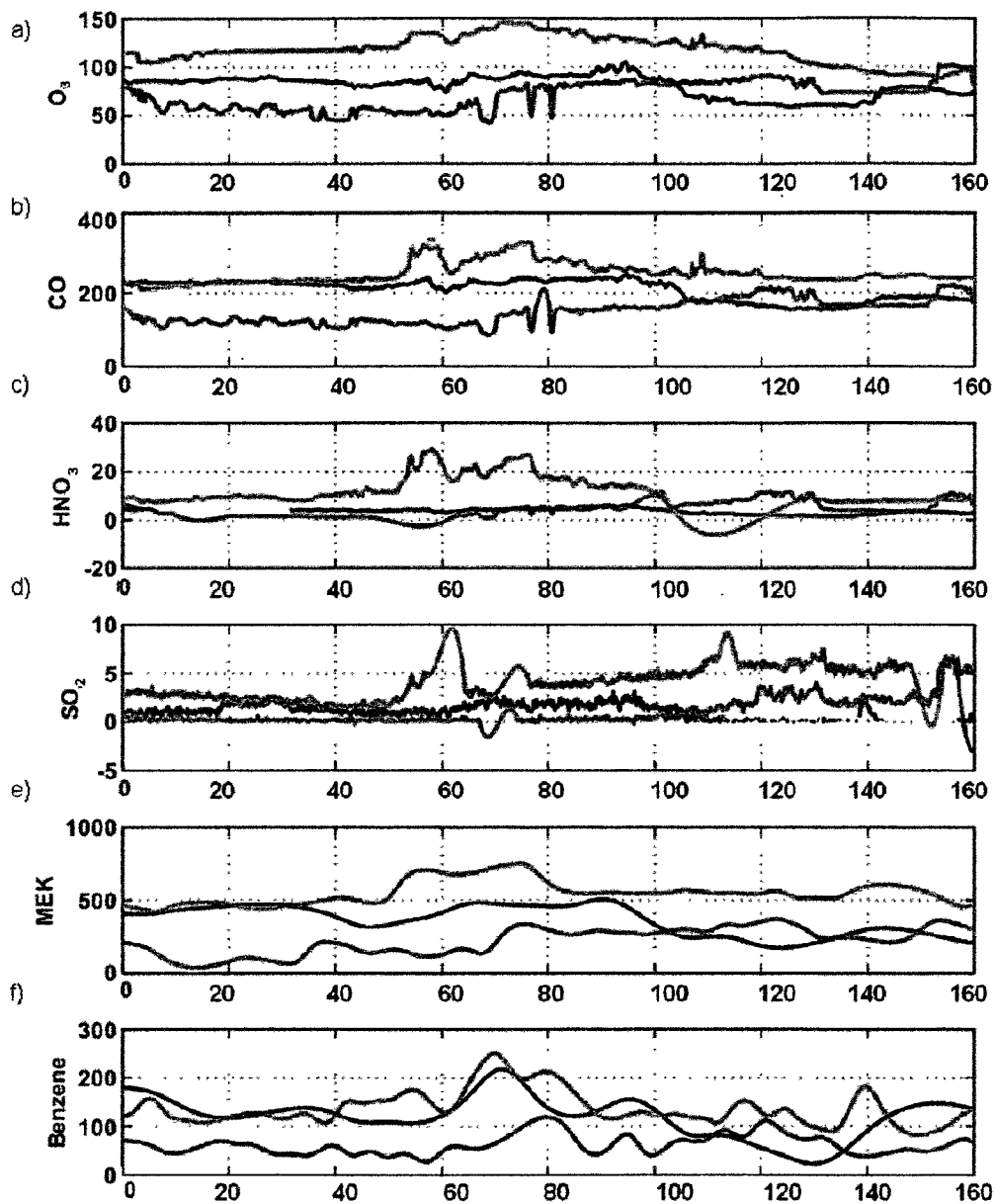
Figure 2.9. Trace gas observations in ppbv of a) O_3, b) CO, c) HNO_3, d) SO_2, e) MEK and f) Benzene within the NYC plume layer as observed in horizontal transect performed by the P-3 on 7/21 and 7/22. Cyan lines designate the coastal GOM transects and magenta lines the open ocean GOM transects on 7/21. Black lines designate observations made during a transect over the central GOM on 7/22.

degrees of spatial variability and with two distinct regimes being apparent over the coastal and open ocean waters. As shown in Figures 2.8a-b, O_3 and CO of the 7/20 plume varied significantly, even over short spatial intervals. Within the same southern GOM transect discussed earlier, CO mixing ratios oscillated 160 ppbv about a mean value of 205 ppbv, and O_3 ranged +/- 70 ppbv about a mean value of 117 ppbv. Similar behavior was observed in HNO_3, SO_2, MEK and Benzene (Figures 2.8c-f). In comparison, wide fluctuations in trace gas mixing ratios over the western GOM-open Atlantic suggested lower values but characterized similar behavior. Mixing ratios of CO were generally below 200 ppbv with O_3 and HNO_3 correspondingly less than 100 ppbv and 12 ppbv respectively.

The high degree of spatial heterogeneity in the mixing ratios appeared to be a direct result to the persistent turbulence inherent to the IBL structure. Despite this near static appearance of the physical state of the plume layer observed on 7/21, frequent variations in vertical wind velocities (Figure 2.8d) were recorded in each of the transects made in the plume as well as isolated peaks in TKE, indicating instances of turbulent activity. To some extent this was expected, with previous works firmly establishing that similar turbulent features and inherent characteristics of the growth of an IBL as a balance between the mixing of cool air by turbulence generated through shear driven TKE and an increase in the stable stratification due to buoyancy driven heat-loss to the surface is ultimately achieved (Garrett, 1987). As previously mentioned the impacts of an IBL on surface mixing ratios of O_3 around the GOM has been explored in a number of works, yet none have captured the full magnitude and scale of the IBL-turbulence impact on a passing airmass' as seen in the aircraft observations of the 7/20 plume.

3.3.2. (7/22~Day 3)

In the absence of new synoptic influences entering the GOM, the IBL-like structure surrounding the plume remained nearly constant throughout day 3 of the plume study. As seen in Figure 2.8, horizontal transects made within the plume layer on 7/22 observed that the majority of its physical characteristics remained unchanged. As on 7/21, winds maintained a southwesterly flow (a mean 230° in direction) within the layer, with the only exception being an average 2m/s increase in wind speed on the 22nd. This increase contributed to increased vertical shear in wind speed within the plume and adjacent lower tropospheric layers, and facilitated the continued low R_i values (Figures 2.7f and l) well below the critical level, thus indicating frequent shear-driven turbulence and a higher probability of enhanced mixing on 7/22.

These conditions continued to have considerable impact on trace gas mixing ratios and chemical processing rates within the plume that day. As suggested in Mahrt et al (1999) and Dacre et al. (2007), the overturning motion is pervasive throughout similar low altitude plumes/IBL layers and contributes significantly to the transit of the plume as well as mixing within it. On 7/22, this appeared to be realized as more concentrated elements of the plume arrived from upwind. Aircraft observations also provided evidence of mixing with recent emissions over the GOM, particularly in the coastal region. As seen in horizontal transects of the plume on 7/22 (Figure 2.9), the primary trace gas species retained their high spatial variability. On average, 20% higher mixing ratios were observed, as CO mixing ratios approached 400 ppbv and O_3 exceeded 100 ppbv. However, NOy remained relatively unchanged at ~6 ppbv with fresh emissions mixing
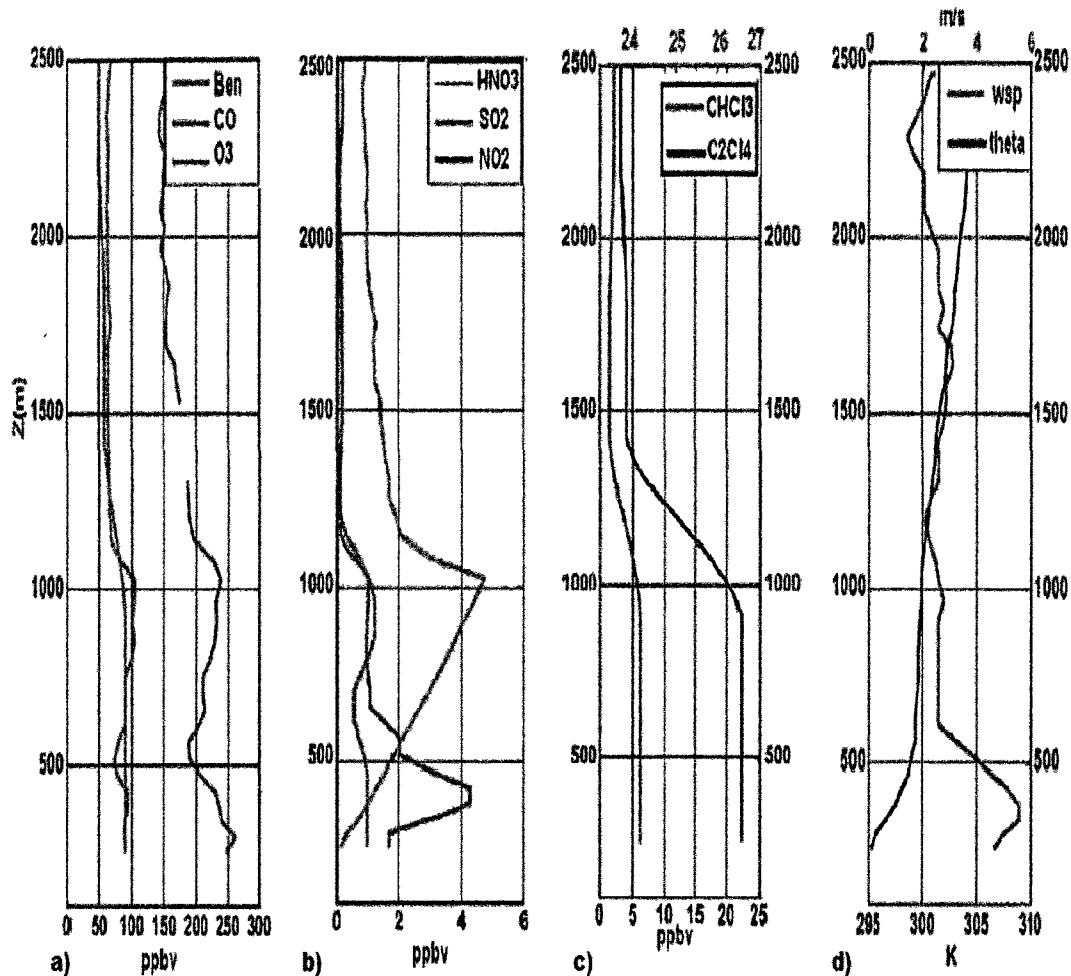
Figure 2.10. Cross-platform observations of the plume by the NASA DC-8, Shown are profiles of a) primary trace gas mixing ratios of O_3, CO and Benzene as well as b) HNO_3, SO_2, and NO_2. Profiles of signature halocarbons CH_3Cl_2 and C_2Cl_4 are shown in c) With physical parameters of wind speed and potential temperature in d).

into the plume and reduced deposition resulting from the detached nature of the plume's transit.

The third day of the plume study provided a unique cross-platform look at the plume with both the P3 and DC-8 intercepting it over the GOM. These encounters observed the trace gas enhancements clearly in relation to the plume's vertical structure.

Profiles by the DC-8 over the western GOM on 7/22 are shown in Figure 2.10, and compared closely with the corresponding profiles by the P-3 presented in Figures 2.6 and 2.7. The vertical distribution of the halocarbon species used in tracking the plume was further seen in the DC-8 observations as well. Particularly evident were the enhancements in $CHCl_3$ (16pptv), CH_3CCl_3 (24 pptv), C_2Cl_4 (23 pptv), and CH_2Cl_2 (52 pptv).

Much of the enhancement in key species mixing ratios resulted from processing within the plume and mixing with fresher emissions. In particular, the enhancement in ozone mixing ratios appeared to be a function of the sustained reduction in O_3 loss facilitated by the IBL structure. As seen in Figure 5, the plume O_3/CO ratios increased substantially from their source region values on 7/20 and particularly on 7/21 where the O_3/CO ratios exhibited best fitted slopes of 0.38 and 0.41 respectively. While these slopes were constant over the coastal waters on both days, a decrease from 0.41 to 0.34 was observed farther out to sea. This difference was one indication that lateral mixing may have occurred between the plume and local airmasses over the coastal region between 7/21 and 7/22. This was further suggested from significant changes in the O_3/NOy ratios which, over the same period, showed a significant rise over the coastal region and a substantial decrease towards the open ocean.

3.4 Inland and Trans-Atlantic Impacts of NYC Plumes

The initial impact of the plumes passage was observed on surface conditions around New England and evolved over the course of 3 days (7/21-7/23) as seen in the times series of trace gas observations made at the three AIRMAP stations (Figure 2.11). As shown, initial detection was made along the coast, where the plume arrived at AIS

40

and TFR in a sequence of peaks in mixing ratios between 7/21 and 7/22. The first of these was sharp rise to 88 ppbv in O_3 at AIS between 1800Z on 7/20 and 0600Z on 7/21 with a coincident elevation to 63 ppbv at TFR. These were accompanied over the same interval by a similar enhancement of the CO mixing ratios, reaching 190 ppbv and 280 ppbv at AIS and TFR respectively. Analysis of hourly canister observations at AIS and TFR showed enhancements coincided with elevations in halocarbon species used to track the NYC plume (Figure 2.11 c and d). These observations further captured the oscillating nature of the arrival of the plume indicated by higher levels of halocarbons at TFR than AIS as seen in Figure 2.11c. This may be derived from increased mixing experienced by the plume as the plume progressed inland. Such phenomena has been observed between AIS and TFR during the New England Air Quality Study (NEAQS) of 2002 (Darby et al., 2006) as well as in the investigation of extreme ozone episodes in the summer of 2001 (Mao and Talbot, 2004a).

Further inland, a lag of 3-6 hours in the detection of the plume was observed at CSP. The inland arrival of CO from the plume manifested as monotonic increase until the morning of the 22nd when levels at CSP peaked at 395 ppbv. Ozone at the CSP showed a similar phase lag with the coastal observations, while the influence of the plume on the observed O_3 mixing ratios at CSP was seen as a significant enhancement in its diurnal cycle. O_3 mixing ratios observed at 1200Z on July 22 at CSP equaled the highest observed that summer, representing the regional impact of the plume. During the plume's passage, CO mixing ratios at AIS, TFR, and CSP exceeded the 90th percentile of levels measured between May 1, 2004 and September 1, 2004. This was also the case for the observations of O_3 and SO_2.
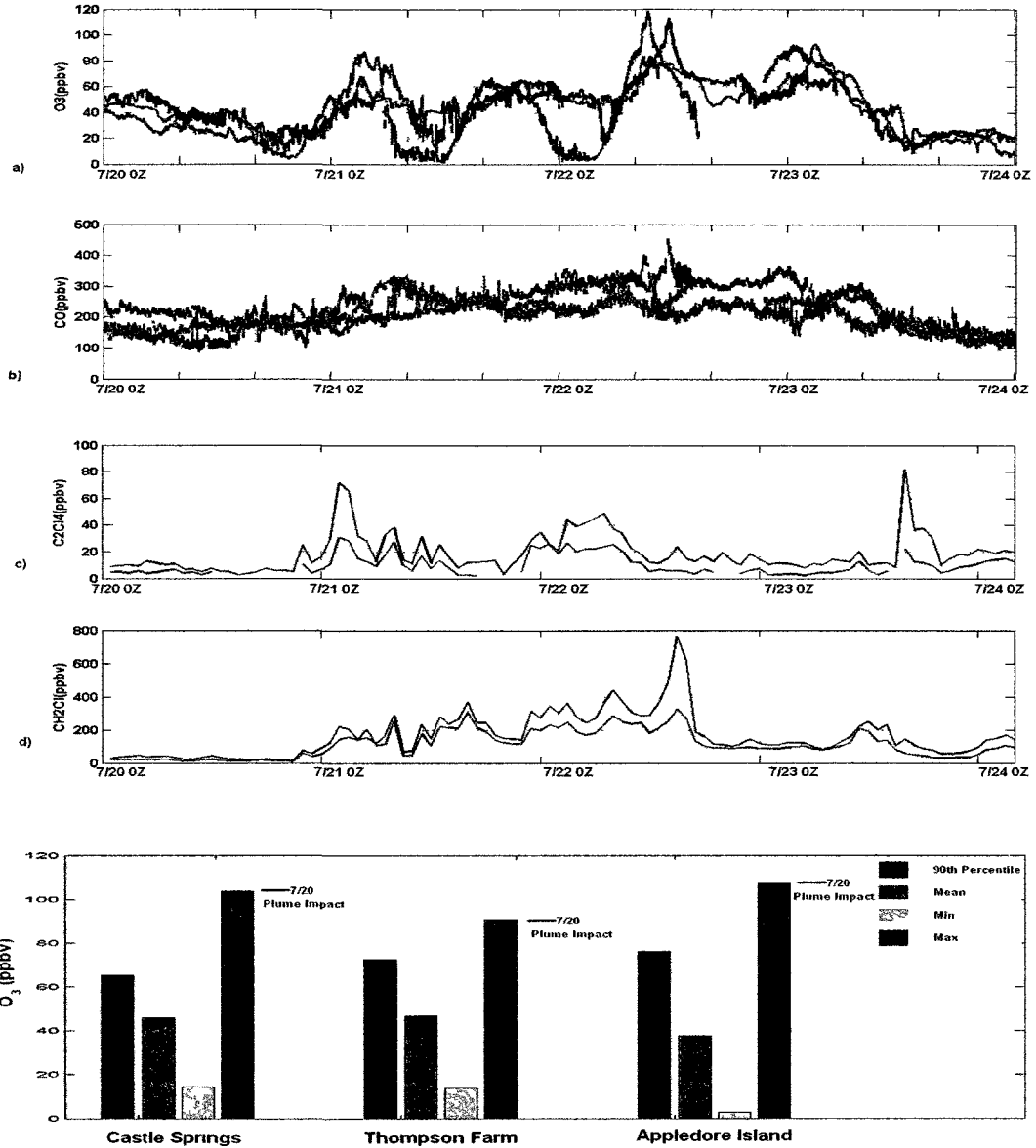
Figure 2.11. Surface observations from the ICARTT campaign and observation statistics for the summer of 2004. Shown are measurements of a) O_3 and b) CO at three AIRMAP stations: TFR (red), AIS (green), and CSP (blue). Canister observations of c) C_2Cl_4 and d) CH_2Cl taken at TFR and AIS are also shown for the same time period. Statistics of the surface O_3 (in ppbv) for the summer of 2004 and the relative impact of the 7/20 plume are presented in d). Green lines indicate the peak values observed at each station during the 7/20 plume's influence which were equivalent to the maximum values measured at each station that summer.

42

Date	7/9	7/11	7/15	7/20	7/25	7/31	8/3	8/7
O3 (ppbv)	80	85	122	150	93	98	105	163
CO (ppbv)	190	160	298	398	220	205	225	390

Figure 2.12. a) HYSPLIT model trajectory for the 7/20 plume (blue) upon leaving the GOM on 7/22 and b) model altitudes. Also shown are model trajectories for similar plumes encountered by the P3 over the GOM on 7/9, 7/11, 7/15, 7/25, 7/31, 8/3, and 8/7. c) 90th percentile values of O_3 and CO observed within these other potential LLO plumes observed by the P3 over the GOM are reported.

43

One remarkable aspect of the 7/20 NYC plume, was not only the quasi-lagrangian manner in which it was observed between NYC and the GOM, but also that its transit and impact were eventually measured over the United Kingdom. Upon leaving the GOM, forward trajectories computed by the HYSPLIT model indicated its continued flow along a southwesterly course across Nova Scotia, Newfoundland as seen in Figure 2.12. By 7/25, these model trajectories tracked theplume to the west coast of Ireland and the British Isles, all while transiting within the lower marine troposphere. This trajectory and timeline was confirmed by intercepts of the plume of the western UK on 7/25, as detailed in Real et al. (2007). Further analysis of the plumes transit within the lower marine troposphere was also explored in this work, with the aid of the UKMet's lagrangian model analysis as detailed in Metven et al, 2006.

This low level means of outflow achieved by the 7/20 plume study raises significant questions as to the frequency and impact of similar plumes across the Atlantic achieved in the lower marine troposphere. While the 7/20 plume was an extreme case within the context of ICARTT 2004, many similar transport events were observed during the course of the campaign. The dates and observed maxima in CO and O_3 mixing ratios recorded within additional low level plumes intercepted over the GOM between 7/15 and 8/07 are indicated in Figure 2.12c. Figures 2.12a and b present the HYSPLIT model forward trajectories for these added encounters, suggesting the possible frequency of 7/20-like plume/outflow events occurring that summer.

4. Summary and Conclusions

In this work, focus has been devoted to a distinct case of LLO that was observed in the GOM region by airborne and surface platforms beginning on July 20th, 2004. This

event was triggered by weak synoptic forcing, and was initially seen as a plume of concentrated industrial and urban pollution vented into shallow tropospheric layers above LIS. In a quasi-Lagrangian manner, multiple intercepts of the plume by the NOAA P-3 were made on subsequent days enabling it to be tracked during transit over the GOM and open western Atlantic waters.

Over the course of a three day quasi-Lagrangian experiment, the 7/20 plume was seen to evolve, with clear linear correlations developing between signature species CO, O_3 and NOy. More specifically, O_3/CO relationships were consistently indicative of efficient photochemical production of O_3. O_3/NOy relationships near the source region showed signs of fresh emissions mixed with photochemically aged air. As the plume arrived in the designated coastal and outflow regions on 21st and 22nd, only the signature of fresh emissions was retained. The close correlation of CO/NO_y contributes to the argument that the plume experienced minimal interaction with the surface over the course of its transit into the GOM and western Atlantic. Much of this detached transit was facilitated by SIBL-like properties of the plume containing layer.

The observation of SIBL-like properties in association with the plume layer in both the coastal and outflow regions is a unique finding that explains much of the efficiency of the 7/20 plumes transport and its eventual impact around the GOM and across the North Atlantic Ocean. On both days of the plume's transit across the GOM, the SIBL structure facilitated widespread observations of periodic turbulence with the plume layer. This turbulence appeared to drive the high levels of spatial heterogeneity in trace gas mixing ratios observed in the plume layer. Future studies which are fortunate to gather similar Lagrangian data from a transiting plume within an IBL would benefit with

45

micrometeorological measurements more capable of resolving the fine spatial scales of the inherent turbulent structures within them. Such observations would also facilitate analysis of other features that also influence low-level transport in the marine atmosphere in conjunction with SIBLs, including low level coastal jets, internal gravity waves and turbulent eddies. Thus, the observations of the 7/20 plume further motivate efforts to better understand the complex lower atmospheric influences that facilitate and shape plume transport over extended distances.

CHAPTER 3. THE SIBL AND MARINE-ATMOSPHERIC CONTROLS ON TRACE-GAS VARIABILITY IN THE GULF OF MAINE.

Abstract

A coastal stable internal boundary layer (SIBL) was observed over the coastal and central Gulf of Maine regions during fourteen separate research flights by the NOAA WP-3D in course of the ICARTT campaign. In these encounters, the upper and lower bounds of the SIBL were defined by sharp gradients in wind speed, wind direction, water vapor mixing ratio, and temperature. These limits were also marked by local minima in turbulent kinetic energy (TKE), which tended to increase within the SIBL layer itself. As expected, thickness/height of the SIBL varied significantly with fetch, particularly during daytime encounters. However, this variation was less during nocturnal encounters, which also yielded observations of a low level jet within the SIBL layer itself. A review of previous SIBL studies suggested three established expressions may prove useful tools in the prediction and evaluation of the SIBL heights measured during the campaign. Comparisons exhibited some agreement nearshore (0-10km) but at moderate to extreme fetches (15-500km), they consistently underestimated the ICARTT SIBL heights. An empirical power function was fitted to the observed values if SIBL height via a least squares method. Potential mechanisms responsible for the differences between the empirical fit/observed SIBL heights and previously established expressions were then explored.

1. Introduction

The analysis of the NYC plume transit made in Chapter 2 clearly established that lower marine tropospheric dynamics are not only crucial for the ventilation of boundary layer pollutants, but also for influencing their long range transport as well. This chapter extends that effort, presenting a further investigation of key lower marine tropospheric influences on trace gas behavior as observed during the ICARTT campaign. Particular focus is given to the persistence of a stable internal boundary layer (SIBL). While this feature was observed during the transit of the NYC plume, it was also consistently detected in the majority of the low altitude aircraft observations made over the coastal and central GOM regions during the campaign period, and is the focus of the research presented in this chapter. Specifically an analysis of the variability and characteristics of the SIBL is pursued, with attention given to the feature's behavior during both day and nighttime regimes. Consideration of the influence of the SIBL as a controlling mechanism on the vertical mixing of trace gases was evaluated as well as its bearing on low-level continental outflow. This includes the facilitation of pollutant transport via an observed nocturnal low-level jet and frequent instances of Kelvin-Helmholtz instability within the SIBL. In broader terms, the numerous observations of SIBL height were also evaluated with respect to theoretical/empirical relationships derived for SIBL phenomena in previous studies. Results from this analysis were further employed in comparison to a simple empirical relationship derived from the data. These efforts were also extended to map out a more accurate physical relation for the SIBL growth in the context of the ICARTT/GOM data and to better characterize underlying mechanisms for frequent SIBL development in the region.

An analysis of SIBL phenomena necessarily begins with consideration of the pronounced static stability which prevails over the North Atlantic in summer months. This characteristic is established through strong stratification, one of the most salient characteristics of the summertime North Atlantic MABL, as low sea surface temperatures (SST) cool near surface layers and maintain static stability under most synoptic conditions (Roll, 1965). Angevine et. al. (2006) recently examined this structure and the processes leading to the formation of a highly stable MABL over the GOM. Within six weeks of ship launched balloon soundings, they observed remarkably similar profiles in the lowest 1-2 km of the coastal atmosphere. Yet, as this study noted, the coastal processes varied significantly with flow patterns and time of day. Specifically, mid-day and afternoon outflow exhibited a deeper mixed layer and therefore greatest transformation as it left the New England coast and entered the marine atmosphere. Within 10 km of leaving the coast, it was estimated that the outgoing air mass experienced a cooling of 5-15 K and contributed to the formation of a newly formed stable layer 50-100 m above the surface. This significant cooling results in a discontinuity in the surface convective fluxes, and often the formation of a thermal internal boundary layer (TIBL) as continental airmasses are advected into the marine boundary layer/lower marine troposphere. A schematic of this process is shown in Figure 3.1.

Thermal internal boundary layers are one form of internal boundary layer created by flow over surface discontinuities. Based on the strong static stability over North Atlantic, the term TIBL is often used interchangeably in the literature with the designation SIBL used here. Measurements of SIBLs and their influence over the local atmosphere over the GOM have been made more than six decades, beginning with a
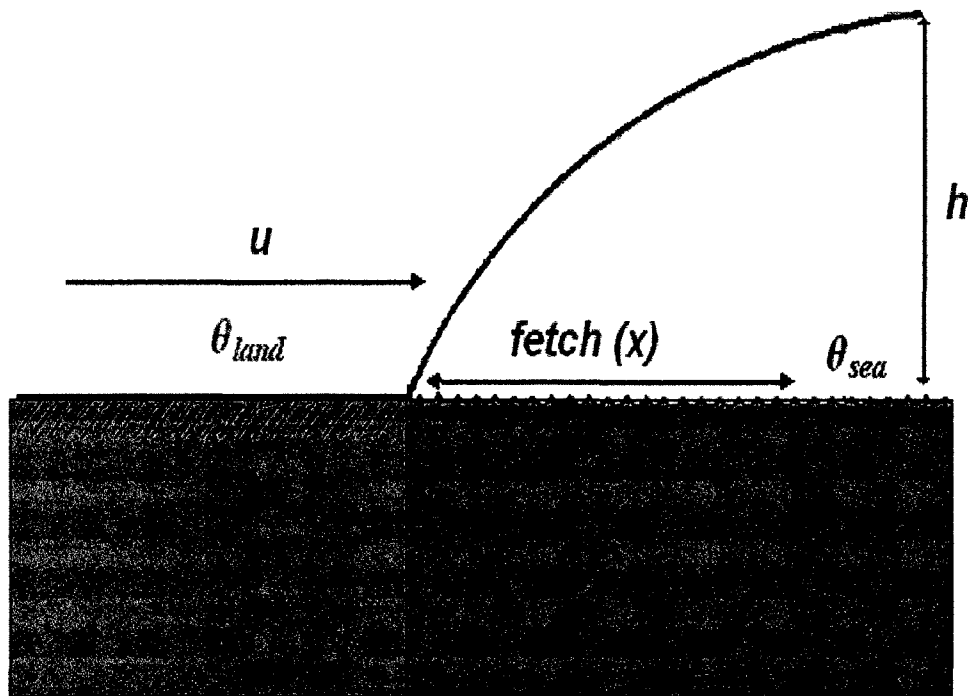
Figure 3.1. Schematic diagram of a coastal thermal (stable) internal boundary layer, developing in the scenario of warm continental air at temperature θ_{land} advected out by prevailing wind of speed u over a colder sea at temperature θ_{sea}. The SIBL height, h, can then be expressed as a function of fetch from shore, x.

series of studies by Craig (1944, 1946) and Kerr (1951). In efforts to predict the SIBL

heights over Massachusetts Bay, Mulhearn (1981) advanced an early analytical

expression for SIBL heights in the region, where SIBL height (h) could be estimated as a

function of fetch (x) from land. Angevine et al (2006) discussed the application of

similar relationships over the GOM, adopting an empirical expression from Garratt

(1992). However, the authors found Garratt's expression underpredicted SIBL heights

during the 2004 ICARTT campaign, and was consequently of limited application in evaluating SIBL influences on trace gas behavior.

Indeed, the impact of SIBLs on trace gas behavior around the GOM region has received attention in a growing number of studies made in the past fifteen years. Gong et al (2000) observed the propagation of internal gravity waves within a shallow SIBL to enhance vertical mixing of O_3 at Chebogue point during the NARSTO-CE 96 field experiment. Angevine et al.(1996) and later Mao et al. (2003) both observed the maintenance of a nocturnal low level jet over GOM waters during enhanced ozone episodes in northern New England, an atmospheric phenomena frequently fostered by the presence of and SIBL. More recently, low-altitude intercepts of coastal power plant plumes by Brown et al (2007) found boundary layer vertical gradients of relative humidity and aerosol surface consistent with SIBL patterns. These observations were also highly correlated with steep gradients in N_2O_5 hydrolysis, thus having direct bearing on the lower atmospheric transport or loss of O_3 and NO_x. Fairall et al (2006) presented similar findings, determining that internal boundary layers formed near the coast were responsible for significantly reduced vertical fluxes of O_3 and a general lack of vertical exchange with the near-surface and overlying layers over the GOM throughout the ICARTT campaign. These authors also observed numerous instances of shear driven turbulence over the GOM, with R_i values in the lower 1000 m frequently dropping below the critical 0.25 level.

It has thus been the focus of this work to pursue the further investigation of the coastal SIBL, as frequently observed over the GOM and its influence upon trace gas variability as well as plume transit. Details of the aircraft and surface observations used

51

during the extensive number of SIBL encounters are described in Section 2. Also within this section, three established expressions for SIBL development are described. Section 3 presents a detailed analysis of the SIBL structure at near and extended fetches from shore. This includes an evaluation of significant differences between daytime and nocturnal behavior of the SIBL, as well as the observation of prominent SIBL-related features, such as the nocturnal low level jet. Final stages of the analysis engage in an evaluation of established analytical expressions for SIBL height in relation to the ICARTT/GOM observations. Final remarks and conclusions drawn from the analysis are presented in Section 4.

2. Methodology

2.1 Observational Data

Observations from the NOAA WP-3D as configured during the ICARTT campaign were used in similar fashion to that described in Fehsenfeld et al. (2006) and detailed further in Chapter 2. Trace gas and meteorological parameters over on land were observed through the AIRMAP regional network previously described as well. Additional observations of sea-surface conditions across the GOM were obtained from the National Data Buoy Center (NDBC) network. Specific buoys used included Station 44007 located at 43.531N, 70.144W (Portland, ME); Station 44013 located at 42.346 N, 70.651W (Boston Harbor); and Station 44005 located at 43.189N, 69.140W (central GOM).

Further parameters that were calculated and employed include virtual potential temperature (θ_v), the gradient Richardson Number (R_i), and turbulent kinetic energy

(TKE) as cited in chapter 2. The additional parameter of the Brunt–Väisälä frequency N was used where:

$$N = \sqrt{\frac{g}{\theta} \frac{\delta\theta}{\delta z}}.$$

(3.1)

Here θ is potential temperature, g is the local acceleration of gravity, z is altitude, and $\frac{\delta\theta}{\delta z}$ describes the stratification of the layer. N is then the natural frequency and at which an air parcel oscillates after being displaced from its original vertical position. This parameter was used to gauge changes in buoyancy and stability in the vertical profiles made through the SIBL, with $N^2 > 0$ implying stable stratification and conversely $N^2 < 0$ indicative of unstable stratification within the observed layer.

2.2 Internal Boundary Layer Expressions

Sutton (1934 and 1953) showed that the diffusion equation applied to flow offshore could take the form

$$u\, \partial\theta/\partial x = K\, \partial^2\theta/\partial x^2$$

(3.2)

where K is a constant eddy diffusivity, u is the wind velocity at the top of the SIBL and $\partial\theta/\partial x$ is the temperature gradient moving from shore to sea. The solution of this then took the form:

$$\theta - \theta_0 = (\theta_i - \theta_0)\, erf\left(z\left(\frac{u}{4}Kx\right)^{1/2}\right)$$

(3.3)

53

with z the aerodynamic roughness of the sea surface, and *erf* is the well known error

function $erf = \dfrac{2}{\sqrt{\pi}}\int_0^x e^{-t^2}\,dt$. Sutton further advanced that under the assumption of

stationarity, this solution could be simplified to:

$$h = 0.18\left(Kx/u\right)^{1/2}.$$ (3.4)

Here, three modified forms of Sutton's expression for SIBL height (*h*) were

employed for evaluation of observed SIBL heights. These expressions were chosen based

on the similarity of their origin to North Atlantic conditions and their ubiquity in SIBL

literature. The first of these was advanced by Mulhearn (1981), based on the analysis of

observed profiles of moisture and temperature above Massachusetts Bay. For fetches (*x*)

between 5 and 500 km, the author found that an internal boundary layer height (*h*) could

be represented by the expression:

$$h \cong 0.015u\left[g\frac{\Delta\theta}{\theta}\right]^{-1/2} x^{1/2}$$ (3.5)

where SIBL height (*h*) at distance *x*, could be determined from the wind speed at the stop

of the SIBL, *u*, and the temperature difference between upwind and downwind surfaces,

$\Delta\theta$ (with θ being the mean upwind temperature).

The second expression arose from the evaluation of SIBL behavior in four

separate field campaigns by Hsu (1983). In this, the author employed a more generalized

expression with h dependent only on fetch. For near-shore fetches (20m-8km)

$$h \cong 1.9x^{1/2}.$$ (3.6)

For further fetches (8km-500km), the author observed less convective influence upon

SIBL development and advanced that SIBL height followed a more gradual curve, with

$$h \cong 0.57x^{1/2} .$$
<div align="right">(3.7)</div>

The third and one of most commonly used expression for SIBL growth originated from a study of offshore flows in the Australian coastal atmosphere by Garratt and Ryan (1989). This expression considered the IBL growth in terms of changes in buoyancy described by θ_v:

$$h \cong 0.02u \left[g \frac{\Delta \theta_v - \theta_{vs}}{\theta_v} \right]^{-1/2} x^{1/2}$$
<div align="right">(3.8)</div>

where g is gravitational acceleration and θ_v and u are measured in atmospheric mixed layer over land that flow out onto the sea with surface virtual potential temperature θ_{vs}

3. Results

3.1 The Daytime SIBL

A SIBL was observed emanating from the New England coastline during fourteen individual research flights by the NOAA P3 over the course of the ICARTT campaign. Flight tracks and dates for these encounters are shown in Figure 3.2 with further indication of whether these were day or nighttime missions. Most of the aircraft encounters were made during the initial and final stages of the flights and thus over coastal waters and fetches between 15 and 80 km from the shoreline. However, during flights on 7/31 and 8/11, rare observations of the SIBL and its features at extensive fetches (>400km) were also made.

In each encounter, the SIBL was consistently identifiable by several distinct features in the aircraft data. Representative profiles of daytime encounters derived from

<div align="center">55</div>
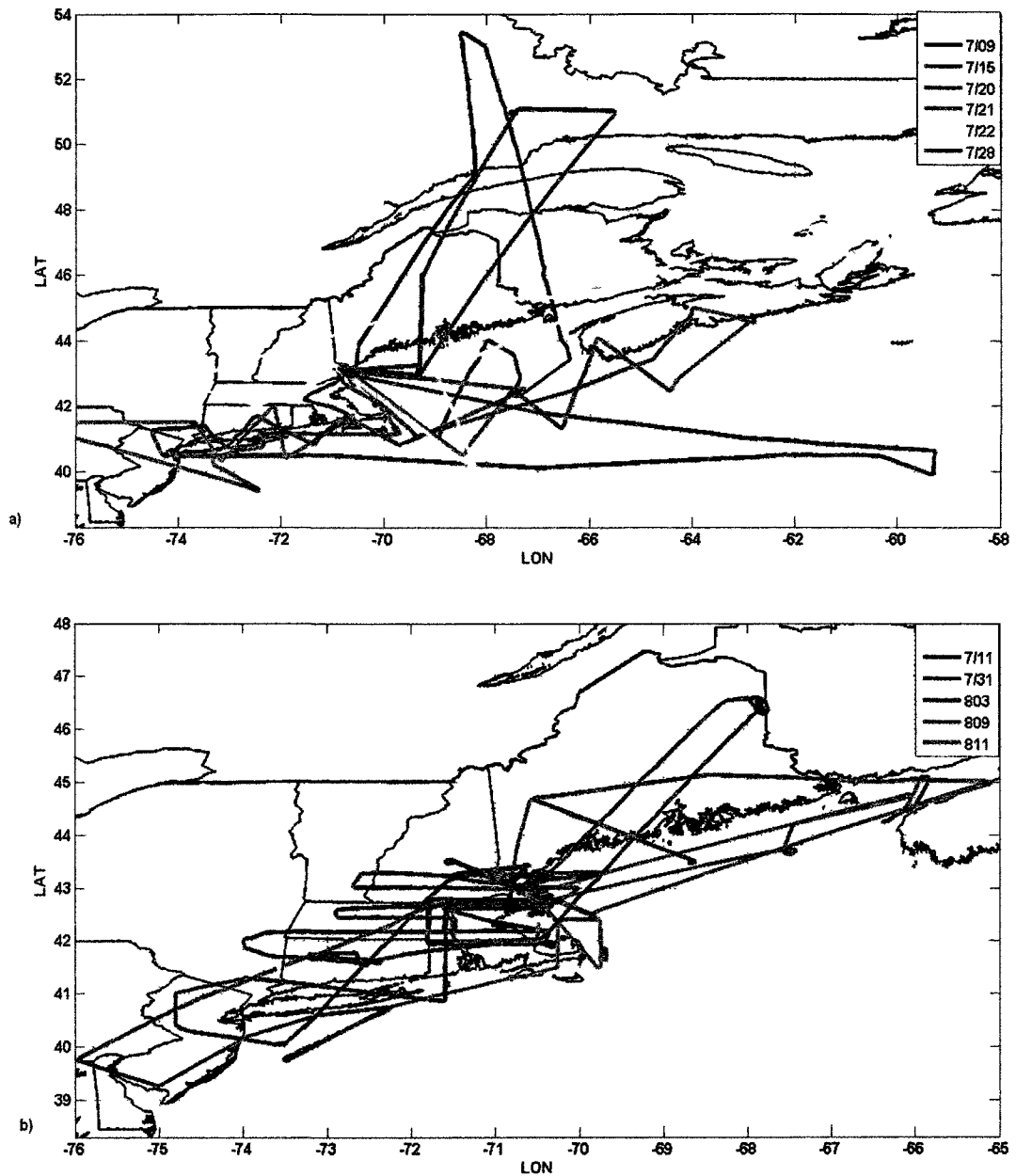
Figure 3.2. Flight paths for NOAA P3 encounters with the SIBL over the GOM. Shown are the dates and tracks for the a) daytime encounters and the b) corresponding nocturnal encounters made by the aircraft.

observations made on 7/09 are shown in Figure 3. In these, it was evident that the top and

bottom of the SIBL layer were bounded by abrupt changes in wind speed, wind direction,

as well as a local minimum in TKE (Figure 3.3e, f, and g). Between these minima, the SIBL was characterized by a significant increase in the water vapor mixing ratio (Figure 3.3d) relative to the overlying layers as well as vertical band of increased TKE, likely signifying Kelvin-Helmholtz (K-H) driven turbulent mixing. This turbulent quality was further suggested by the low Richardson number values (0.02-0.24) sustained throughout the layer (Figure 3.3h).

As in the case of the NYC plume, the greatest difference between the daytime SIBL characteristics at near-shore (fetches <100 km, blue lines) and those further out sea (fetches >100km, red lines) was its height or thickness. This is clear in the July 9th profiles of selected trace gas mixing ratios and physical parameters and shown in Figure 3a-c, where a comparison is presented between the SIBL observed at 37 km from the shore and 160 km further out to sea. Here near-shore thickness suggested by the profiles of CO and SO_2 mixing ratios was roughly 50 m, while at the extended fetch, profiles of the same species indicated a layer thickness of 150 m. The aforementioned mechanical mixing driven by the K-H instability appeared to be the principle mechanism responsible for the difference, as the increase in layer thickness was accompanied by a large increase in the TKE within the SIBL layer observed further out to sea.

This aspect of SIBL growth over the GOM is consistent with some theories of SIBL growth as a function of turbulent fluxes/mixing (Garratt, 1987; Rogers et al, 1995). In these, continental air within the SIBL is mechanically mixed through K-motions, eventually reaching a quasi-equilibrium state with the new marine environment. An increase in TKE accompanies this process, as wind shear increases. This develops into a
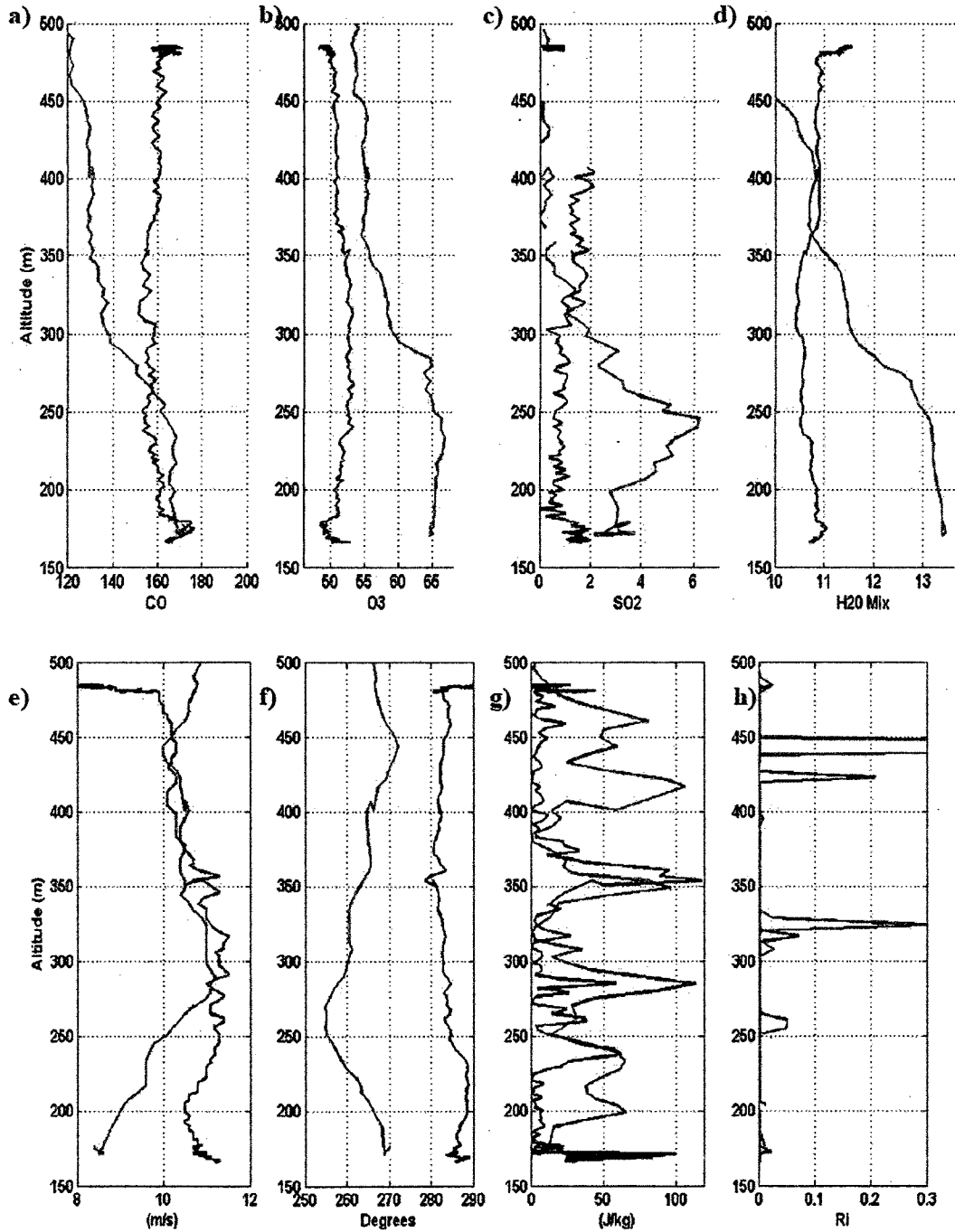
Figure 3.3. Daytime vertical profiles of physical parameters and trace gas mixing ratios observed on 7/09. Shown are observed mixing ratios in ppbv of CO, O_3, SO_2 and H_2O vapor in a)-d) respectively. Vertical profiles of wind speed, wind direction, TKE and R_i are shown in e)-h). Blue lines represent observations at 37km from shore and red lines indicate observed values 160m from shore.
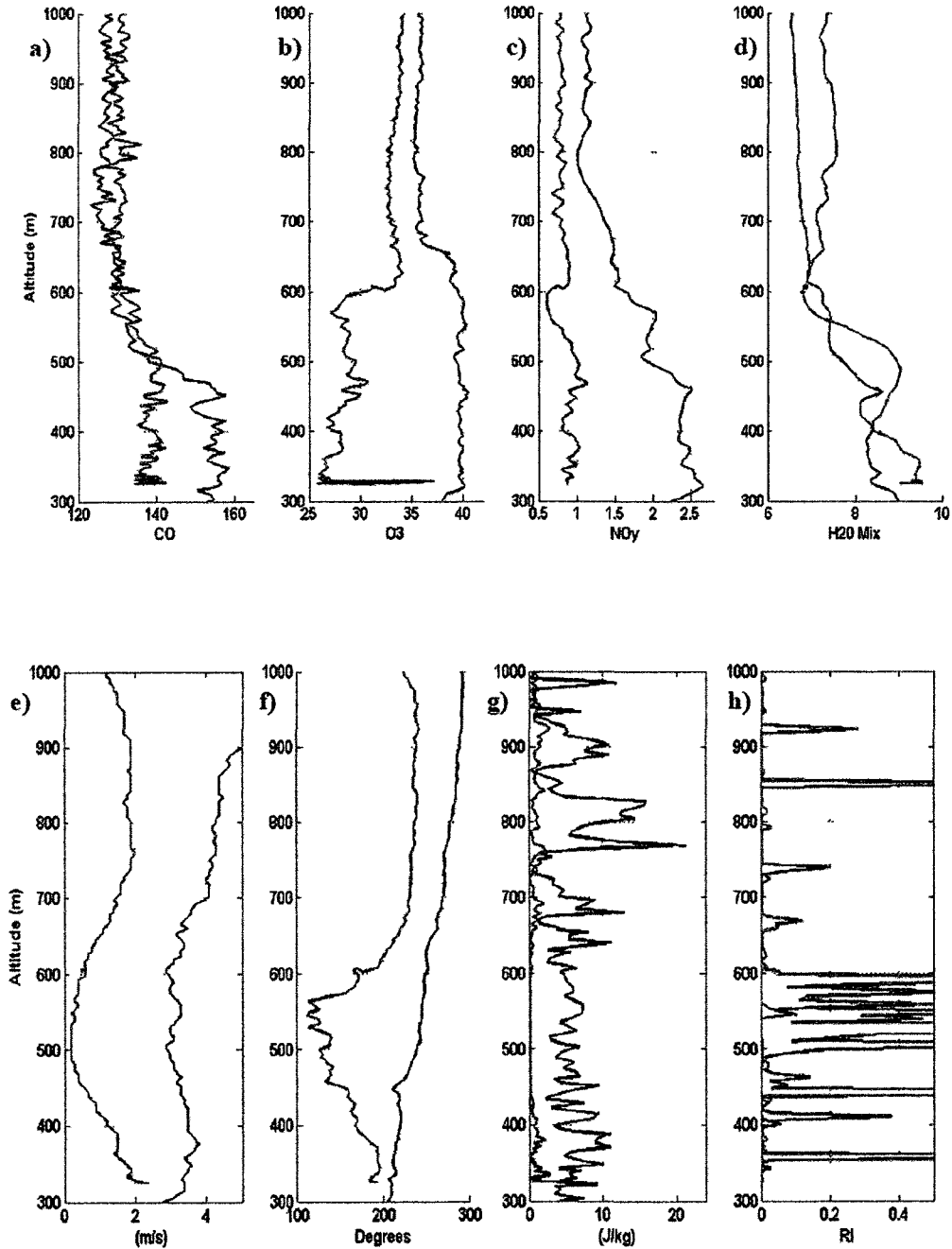
Figure 3.4. Nocturnal vertical profiles of physical parameters and trace gas mixing ratios observed on 7/09. Shown are observed mixing ratios in ppbv of CO, O_3, SO_2 and H_2O vapor in a)-d) respectively. Vertical profiles of wind speed, wind direction, TKE and R_i are shown in e)-h). Blue lines represent observations at 67 km from shore and red lines indicate observed values 130m from shore.

cycle, where stability is decreased, the layer thickened and the process repeated until the surface buoyancy flux approaches zero.

3.2 The Nocturnal SIBL

It was generally observed that the SIBL thicknesses observed during nocturnal intercepts were larger than their daytime counterparts. However, the difference in SIBL thickness was more invariant with fetch during the nocturnal intercepts. Representative nocturnal profiles were taken from observations obtained during the August 7th encounters and are presented in Figure 3.4 where this is clearly evident. In comparison of the profiles of CO and water vapor mixing ratio (Figure 3.4a and 4d), the difference between the SIBL thickness at 67 km and that at 130 km offshore is relatively small. Despite this, the internal characteristics of the SIBL exhibited several key deviations. While low wind speeds (Figure 3.4e) characterized the SIBL in both locations, vertical shear in wind speed was more prominent further out to sea. It can also be seen that at this point that the SIBL layer exhibited greater stability, with R_i values predominantly above the 0.25 value.

Much of the increased nocturnal stability stemmed directly from a reduction in the surface buoyancy fluxes as well as the turbulent fluxes within the SIBL itself. Evidence of this was particularly clear further out to sea, where the magnitude of TKE at night (Figure 3.4h), was at least 80% smaller than that observed during the day. The only exception to this observation was seen during periodic detection of a nocturnal low level jet (LLJ).

Observation of the periodic LLJ was a crucial difference observed between the SIBL feature during the day versus night. As seen in figure 3.5, a clear observation of this feature was made during profiles made on night of August 11th. The defining characteristic of this profile is the smooth gradient in wind speed between 10 and 540m in altitude with a maximum of 19.3 m/s reach at that height (Figure 3.5c). Presence of the LLJ and its inducement of turbulence within the SIBL are further signified by the increased band of TKE seen in Figure 3.5e, which is on the order of 2-3 time greater than the values observed in other day and nighttime encounters. This is consistent with previous studies which have tied level jets to patchy and intermittent shear instabilities observed within the SIBLs. One of the first studies to attribute increased O_3 mixing ratios in the stable layer to turbulence was conducted by Samson (1978), who related localized increases O_3 mixing ratios to a nocturnal LLJ. More recently, studies by Reitebuch et al. (2000), Corsmeier et al. (1997) and Beyrich et al. (1996) confirmed the importance of the LLJ in generating sufficient turbulence to mix O_3 stored in nocturnal residual layers to the surface over periods of several hours.

3.3 Analytical Comparisons

Applying the aircraft observations in conjunction with the AIRMAP and NDBC buoy measurements, predicted SIBL heights were computed using the three SIBL expressions described in section 2.2. The observed/predicted comparison is shown in Figure 3.6, where it can be seen that that the established expressions consistently underestimated the SIBL heights in the GOM in terms of the ICARTT measurements.

A breakdown to daytime and nighttime cases (Figure 3.6b and 3.6c), showed
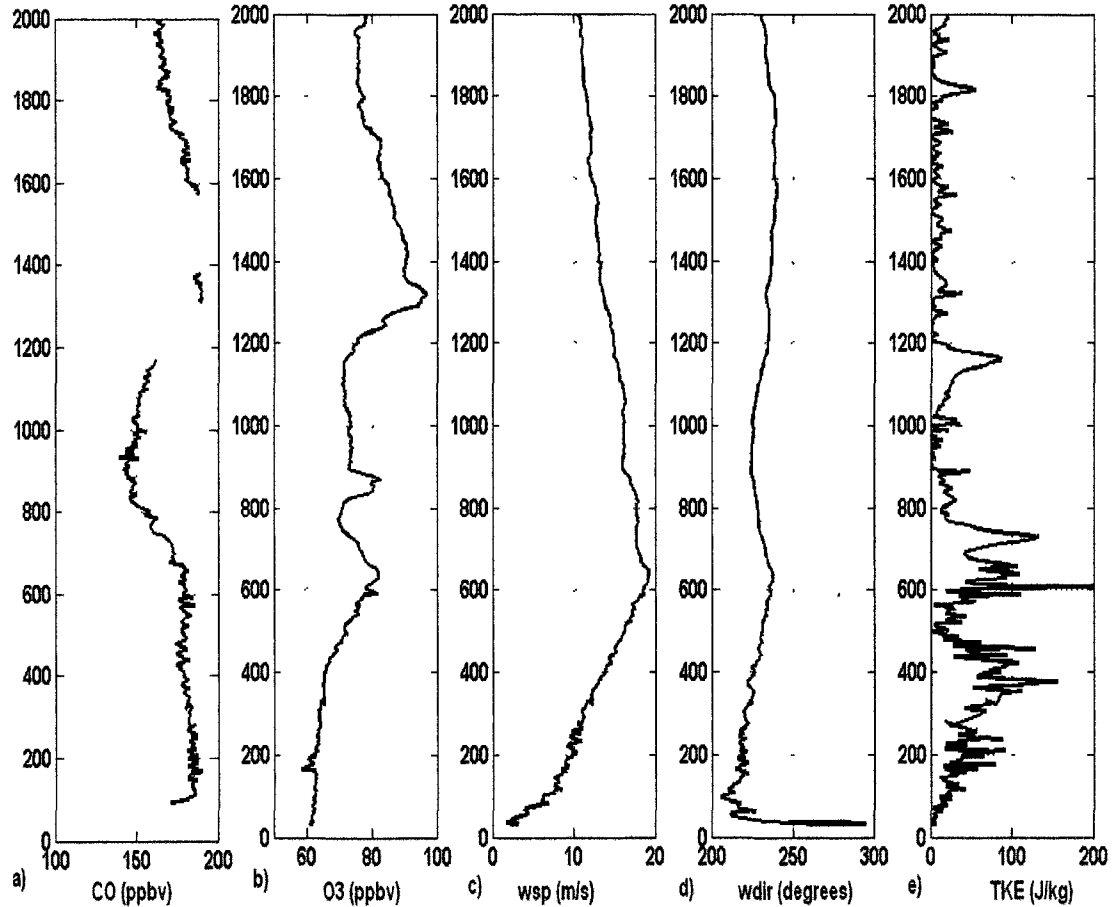
Figure 3.5. Selected vertical profiles of physical parameters and trace gas mixing ratios observed made during the observation of a nocturnal low-level jet within the SIBL on August 11th. Shown are mixing ratios of CO and O_3 in a) and b). Profiles of wind speed, wind direction and TKE are shown in c)-e).

slightly better agreement with the nocturnal observations. Hsu's first generalized expression generated the closest estimates of SIBL heights, with a root mean square (RMS) error between the observed and predicted values of 172 m. Considerably larger RMS errors for the Mulhearn and Garratt predicted values were found, at 426 m and 211 m respectively. It can be seen from the plot of absolute difference between predicted and
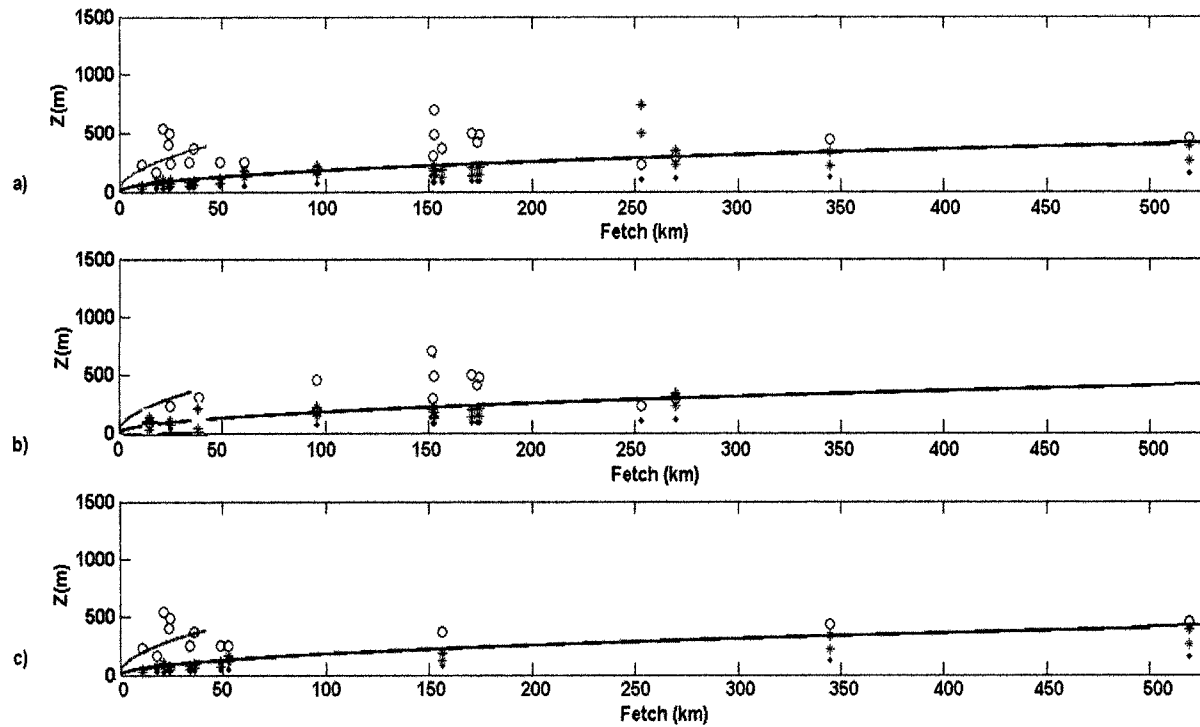
Figure 3.6. Comparisons between observed SIBL heights as observed by the aircraft in the ICARTT campaign and heights calculated from the three established SIBL height expressions taken from the literature. Shown are comparisons for a) day and night combined observations, b) day only observations, and c) night only observations. For all cases, blue circles mark observed heights, red stars represent heights from Mulhearn's relation, black stars heights from Garratt's relation, while the green and blue lines are Hsu's original and corrected formulae.
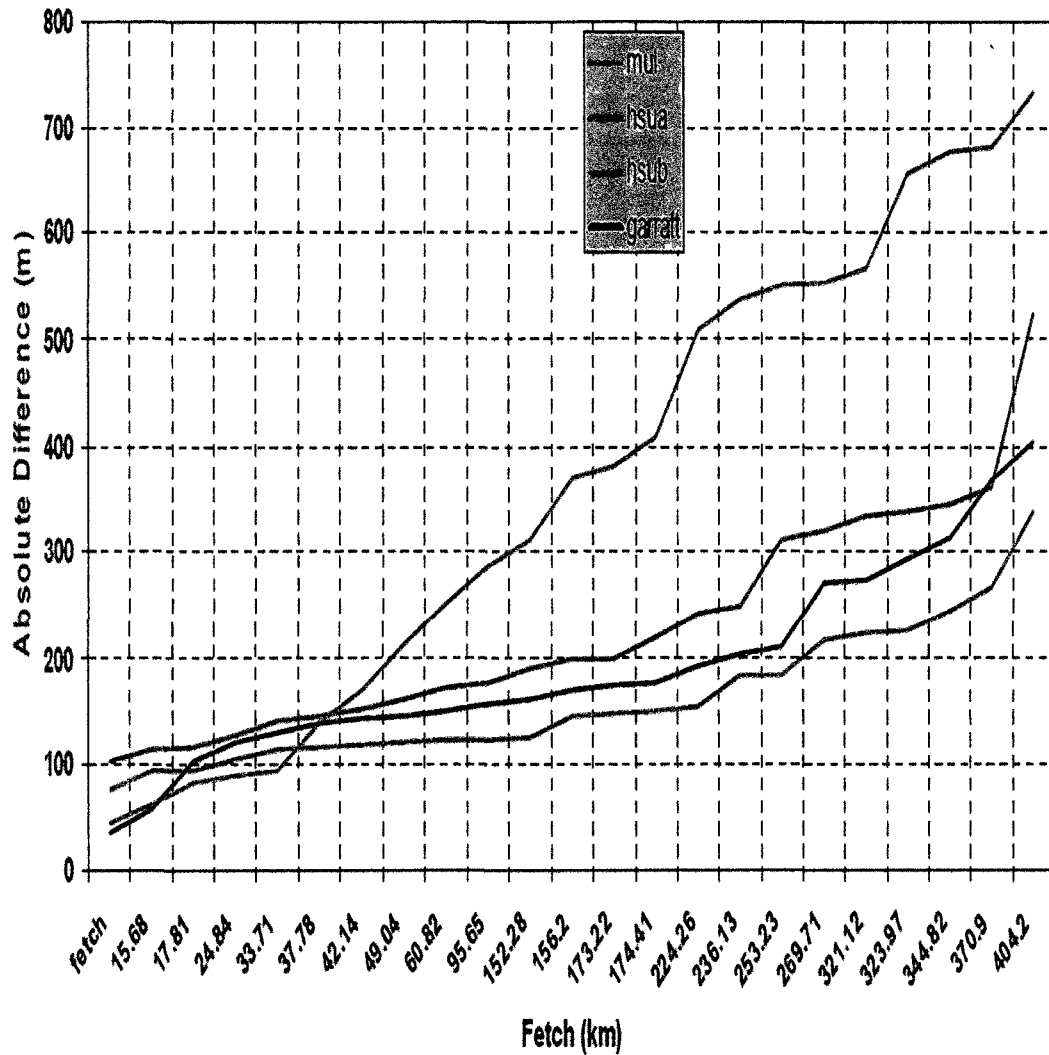
Figure 3.7. Absolute differences between observed and calculated SIBL heights during the ICARTT campaign versus fetch. Shown are comparisons with calculated values using relationships from Mulhearn (red), Hsu and modified Hsu (magenta and cyan), and Garratt (black).

observed values shown in Figure 7 that these large errors/differences increased with fetch. This is surprising, particularly in the case of the Mulhearn expression, derived from data taken above Massachusetts Bay.

Following the comparison with established expressions, a new empirical relationship was derived for the ICARTT SIBL heights. Applying the method of least squares, a simple power fit of the form:

$$h = a \cdot x^b \tag{3.9}$$

to the observed SIBL heights was made. Results of this generated the relation:

$$h = 4.083 \cdot x^{0.37} \tag{3.10}$$

fitted to the 95% confidence level and an R-square of 0.70. The resulting RMSE of this relation was 68 m. The form of this power function fit to the ICARTT SIBL height data over the GOM in essence preserved the SIBL height as a function of $x^{3/2}$ relation set forth by Sutton (1934 and 1953) and subsequently adjusted in many recent studies. Like Hsu's relation (1983) however, this expression is empirical in nature and limited by its lack of consideration of the physical state variables in the lower atmosphere and the nature of the underlying surfaces affecting the flow within the SIBL.

The close correspondence between trace gas distributions and SIBL thickness frequently seen in the ICARTT/GOM observations motivate further concerns the use of a single expression. During the observations made within the daytime SIBL at a 370 km fetch on August 7th (Figure 3.8a) the relationship between SIBL height and mixing ratios appeared very clear. However, upon closer inspection (Figure 3.8b), the SIBL thickness appeared to vary somewhat with species. Specifically, based on the profiles of O_3, SO_2, and HNO_3, an estimated height of 650m would be determined while based on the profiles of CO, a lower height of 540m would be estimated. This variability of height with species was observed more pronounced at shorter fetches where more mixing was observed, and thus made nearshore SIBL height determination cumbersome by this method. It is likely

65

that the effectiveness of using similar trace gas mixing ratio profiles as well as the observation of physical variables would be maximized if used in robust framework/model which considers the dynamical influence of turbulent and convective fluxes on SIBL development. Some works in which this has been pursed include those by Renfrew et al. (2000), Fairral et al (2003) and Rowe et al. (2011).
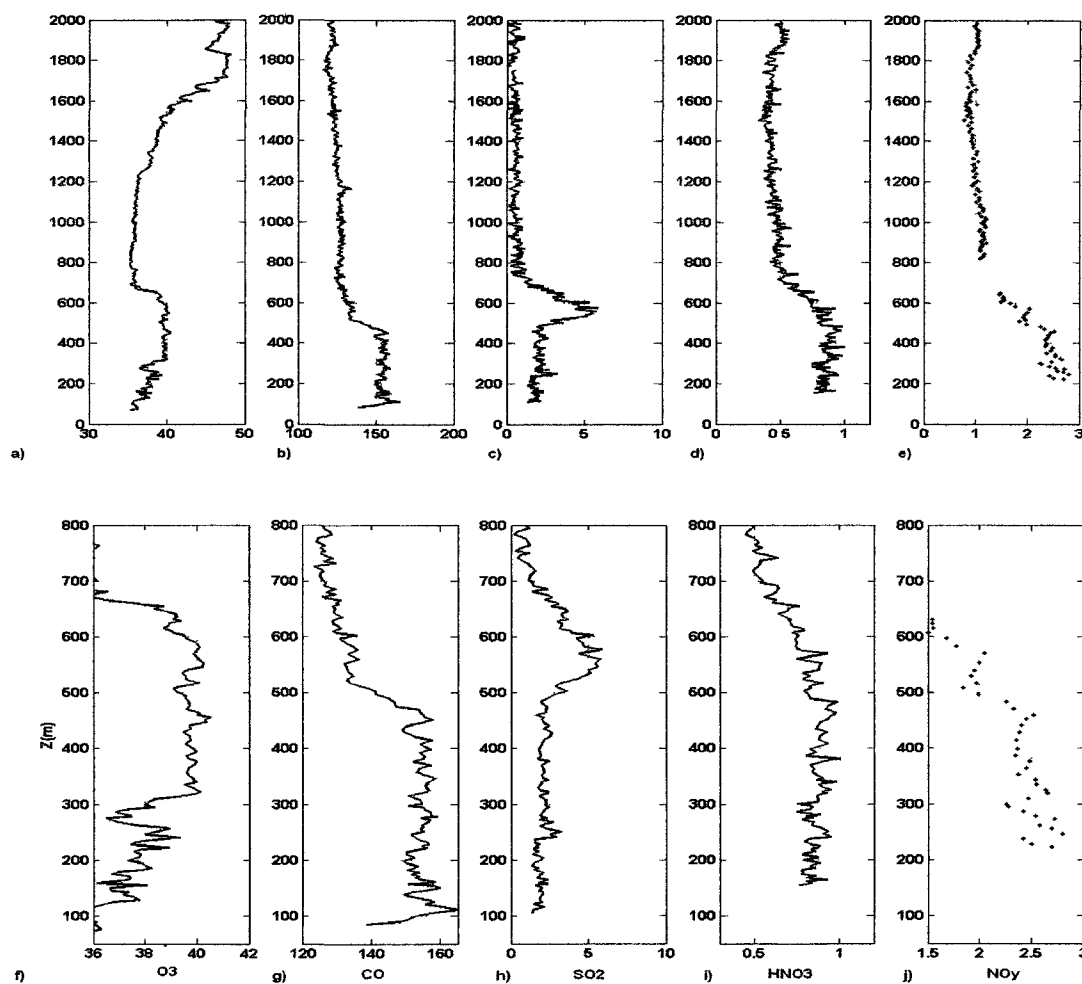
Figure 3.8. Daytime profiles of primary trace gas mixing ratios (in ppbv) during the 8/07 SIBL encounter. Shown are a) O_3, b) CO, c) SO_2, d) HNO_3 and e) NO_y and zoomed in upon for the same profile and species in f) through j).

4. Conclusions

Based on extensive aircraft encounters, the behavior of a persistent coastal SIBL over the GOM was studied during July and August of 2004. It was seen that daytime characteristics such as the height of the SIBL varied significantly with fetch from shore. SIBL height was more invariant during nighttime regimes, but characteristics within the SIBL layer still varied considerably from coastal to more open ocean locations. Strong mechanical mixing generated by shear driven K-H instability was observed, impacting the vertical profiles of trace gas mixing ratios and the overall layer thickness. A nocturnal LLJ was also observed within the SIBL layer, which is a feature that has strong bearing upon the long distance transport of trace gas pollutants over water.

Three established SIBL relations consistently underpredicted the SIBL heights during the ICARTT period. This suggests that additional influences should be considered in efforts to predict SIBL development in the region. The effect of shear driven turbulence was pervasive in the observations, and thus a very likely influence that should be considered in that regard.

CHAPTER 4. SUMMARY AND CONCLUSIONS

A study of the lower marine troposphere and its influences upon trace gas variability and transport has been presented, with an analysis based largely on the observations obtained during the ICARTT 2004 campaign. Through a preliminary examination of this data, evidence revealed a persistent flow of trace gas pollutants at low altitudes above the Gulf of Maine (GOM) which appeared to contribute to regional air quality episodes as well as low level continental outflow (LLO) over the North Atlantic Ocean. The maintenance of this low level flow throughout the six week summer campaign motivated the central theme of this work: to identify and characterize particular features in the lower atmosphere which strongly shape the evolution and transit the polluted plumes/airmasses over the GOM and the western North Atlantic. In Chapter 2, this was pursued by means of a case study. Specifically, a quasi-lagrangian analysis of a newly emitted plume emanating from New York City was employed. As the plume made its way in low altitude layers over Long Island Sound, into the GOM, and eventually across the entire North Atlantic, it was observed that its transformation and transit were greatly influenced by a stable internal boundary layer (SIBL) formed at the GOM land-sea transition. A more detailed examination of this SIBL and its influences upon trace gas behavior was then made in an ensuing study presented in Chapter 3. Particular findings included that the SIBL significantly influenced the vertical partitioning of trace gas species. This included inhibition of vertical mixing with adjacent layers above and below

the SIBL, enhanced mixing within the SIBL itself, and long range transport achieved by a nocturnal low level jet.

The case study presented in Chapter 2 was based on a series of research flights which provided a nearly unprecedented observation of a plume's transit and transformation over the GOM/North Atlantic. As the chapter related, the specific sequence of the plume's evolution in the lower marine troposphere was discernable, beginning with the plume's origin as a polluted airmass characterized by high levels of industrial and urban species, residing in a residual layer above Long Island Sound. As the airmass was advected northeastward, wind shear and convective cooling from the sea surface below contributed to the plume layer evolution into an SIBL over the GOM. In this, the NYC plume was observed between 100 and 200 m thick over the coastal New England waters and up to four times thicker further out to sea. Parameters such turbulent kinetic energy, the gradient Richardson number, and virtual potential temperature were employed to diagnose constant stability in the atmosphere surrounding the plume, despite the frequent manifestation of shear driven turbulence within the plume layer itself.

The physical characteristics of the NYC plume/plume layers while over the GOM significantly shaped its eventual impact in New England as well as across the North Atlantic. The SIBL structure significantly inhibited vertical exchange with the surface, thereby minimizing loss by deposition and allowing the plume to maintain much of its near-source region signature throughout the days it was tracked. Lateral exchange between the NYC plume and recent emissions from the Boston source region were observed enhancing its heavy industrial/urban trace gas composition and its eventual impact on surface conditions regionally and intercontinentaly. In northern New England,

this impact was extreme, with AIRMAP observations of CO, O_3 and SO_2 exceeding the 90th percentile and reaching the maximum levels of those measured that summer. Lagrangian model simulations projected the NYC plume's course across the North Atlantic and to the west coast of Britain within lower levels of the marine troposphere. This was confirmed in related works, through aircraft intercepts made over the United Kingdom five days later. Further exploration of low-altitude intercepts of additional plumes over the GOM in the summer of 2004 showed that the NYC plume was one of many coastal plumes in the LMT that impacted the surface conditions around northern New England. Based on lagrangian model simulations, it was also seen that these added plume exhibited significant potential for making their way across the North Atlantic as well, contributing to the continental outflow of pollutants to marine and European locations far downwind.

The significant impact of the NYC and related plumes warranted a closer look at the processes shaping its evolution over the GOM. This took the form of a process study of the SIBL during the ICARTT campaign, as presented in Chapter 3. Further analysis of the aircraft data demonstrated that the SIBL appeared to be a relatively consistent feature observed in the majority of low altitude measurements over the coastal and central GOM during the campaign period. It was shown that the SIBL in these encounters maintained many of the characteristics of the SIBL/plume layer seen in the NYC case study. This included the vertical partitioning of trace gas species, minimization of surface influences upon trace gas mixing and removal, as well frequent episodes of shear-driven turbulence. However the addition of nocturnal intercepts revealed that the SIBL height was more invariant with fetch at night. Nocturnal encounters provided observations of a low level

70

jet, facilitated by the SIBL layering and contributing to the extended transit of pollutants at lower altitudes. In broader terms, the SIBL behavior during the ICARTT campaign was consistent with similar phenomena observed in related works. However, established expressions that used in situ observations of temperature, wind speed, and SST to predict SIBL height underestimated the heights observed during the campaign. This discrepancy grew larger as a function of fetch from land and that suggested further parameters should be considered in SIBL height determination over the GOM.

The ICARTT data set provides a unique wealth of information concerning the lower marine atmosphere and the dynamic relationship between the physical features and trace gas behavior therein. It has been the goal of this work to use this data to explore selected cases and phenomena, particularly in their application to regional air quality and low level continental outflow from North America. The general findings of this study strongly motivate further consideration of LLO and its impact on intercontinental air quality episodes as well as the global climate system. More specifically, the analysis advanced here has demonstrated through unique aircraft observations that the nature of LLO events is complex, where the influence of smaller spatial and temporal scales of coastal atmospheric dynamics must be considered. Within the case studies pursued, these coastal influences were manifested in the form of residual layers, stable internal boundary layers, Kelvin-Helmholtz turbulence, and nocturnal low-level jets. Further investigation determined that these features shaped trace gas variability, promoted mixing within plume layers while inhibiting any significant exchange or deposition with the sea surface. Over time scales of several days, it was further evident that these features also contributed to longer distance transport of the pollutant trace gases, and with favorable

synoptic conditions, evolved into large scale outflow events to the western North Atlantic

region and more distant downwind locations across Europe.

REFERENCES

Angevine, W. M., White, A. B., and Avery, S. K.: Boundary-layer depth and entrainment zone characterization with a boundary layer profiler, Bound.-Lay. Meteorol., 68, 375–385, 1994.

Angevine, W.M., Trainer, M., McKeen, S.A., Berkowitz, C.M.: Meteorology of the New England coast, Gulf of Maine, and Nova Scotia: Overview. J. Geophys. Res. 101 (D22), 28893-28901, 1996a.

Angevine, W.M., Buhr, M.P., Holloway, J.S., Trainer, M., Parrish, .D., MacPherson, J.I., Kok, G.L., Dchillawski, R.D., Bowlby, D.H.:Local meteorological features affecting chemical measurements at a North Atlantic coastal site. J. Geophys. Res 101 (D22), 28935-28946, 1996b.

Angevine, W. M., Senff, C. J., White, A. B., Williams, E. J., Koermer, J., Miller, S. T. K., Talbot, R., Johnston, P. E., McKeen, S. A., and Downs, T.: Coastal boundary layer influence on pollutant transport in New England, J. Appl. Meteorol., 43, 1425–1437, 2004.

Angevine, W. M., Hare, J. E., Fairall, C. W. , Wolfe, D. E. , Hill, R. J. , Brewer, W. A., and A. B. White: Structure and formation of the highly stable marine boundary layer over the Gulf of Maine, J. Geophys. Res.,111, D23S22, doi:10.1029/2006JD007465, 2006.

Angevine, W. M.: Transitional, entraining, cloudy, and coastal boundary layers. Acta Geophys 56: 2–20. doi:10.2478/s11600-007-0035-1, 2007.

Atkinson, B. W.: Meso-scale Atmospheric Circulations, Academic Press, London, 1981.

Atkinson, B. W. and Shaub, A. N.: Orographic and Stability Effects on Daytime, Valley-Side Slope Flows, Bound. Lay. Met., 68, 275–300, 1994.

Banta, R. M.: Late-morning jump in TKE in the mixed layer over a mountain basin, J. Atmos. Sci., 42, 407–411, 1985.

Banta, R. M., Senff, C. J., White, A. B., Trainer, M., McNider, R. T.,Valente, R. J., Mayor, S. D., Alvarez, R. J., Hardesty, R. M., Parrish,D., and Fehsenfeld, F. C.: Daytime buildup and nighttime transport of urban ozone in the boundary layer during a stagnation episode, J. Geophys. Res., 103(D17), 22519–22544, 1998.

Banta, R. M., Pichugina, Y. L., and Brewer, W. A., Turbulent velocity-variance profiles in the stable boundary layer generated by a nocturnal low-level jet, J. Atmos. Sci.,

63, 2700–2719, 2006. Barlow, J. F., Rooney, G. G., von Hunerbein, S., and Bradley, S. G.: Relating urban surface layer structure to upwind terrain for the Salford experiment (Salfex), Bound. Layer Meteorol., 127(2), 173–191, 2008.

Barnes, G., Emmitt, G. D., Brummer, B., Lemone, M. A., and Nicholls, S.: The structure of a fair weather boundary-layer based on the results of several measurement strategies, Mon.Weather Rev., 108, 349–364, 1980.

Batchvarova, E. and Gryning, S.: Applied model for the growth of the daytime mixed layer, Bound.-Lay. Meteorol., 56, 261–274, 1991.

Bennartz, R.: Global assessment of marine boundary layer cloud droplet number concentration from satellite, J. Geophys. Res., 112, D02201, doi:10.1029/2006JD007547, 2007.

Berkowitz, C. M., Fast, J. D., and Easter, R. C.: Boundary layer vertical exchange processes and the mass budget of ozone: Observations and model results, J. Geophys. Res., 105, 14 789–14 805, 2000.

Beyrich, F., Weisensee, U., Sprung, D., Gusten, H.: Comparative analysis of sodar and ozone profile measurements in a complex structured boundary layer and implications for mixing height estimation. Bound. Layer Meteorol., 81, 1–9, 1996.

Brasseur, G., Orlando, J. J., and Tyndall, G.: Atmospheric chemistry and global change, OUP, Oxford, 1999.

Brasseur, G. P., Prinn, R. G., and Pszenny, A. A. P.: The Changing Atmosphere. An integration and Synthesis of a Decade of Tropospheric Chemistry Research, in: Global Change – The IGBP Series, Springer, Heidelberg, 2002.

Brough, N., C. E. Reeves, Penkett, S. A., Stewart, D. J., Dewey, K., Kent, J., Barjat, H., Monks, P. S., Ziereis, H., Stock, P.,Huntrieser, H., and Schlager, H.: Intercomparison of aircraft measurements on board the C-130 and Falcon over southern Germany during EXPORT 2000, Atmos. Chem. Phys., 3, 2127–2138, 2003.

Brown, S. S., T. B. Ryerson, A. G. Wollny, C. A. Brock, R. Peltier, A. P. Sullivan, R. J. Weber, J. S. Holloway, W. P. Dubé, M. Trainer, J. F. Meagher, F. C. Fehsenfeld, and A. R. Ravishankara : Variability in nocturnal nitrogen oxide processing and its role in regional air quality, Science, 311, 67-70, 2006.

Burk, S. D. and Thompson, W. T.: The summertime low-level jet and marine boundary layer structure along the California coast, Mon. Weather Rev., 124, 668–686, 1996.

Businger, S., Johnson, R., Katzfey, J., Siems, S., and Wang, O.:Smart tetroons for Lagrangian air-mass tracking during ACE 1, J. Geophys. Res., 104, 11 709–11 722, 1999.

Caughey, S. J., Wyngaard, J. C., and Kaimal, J. C.: Turbulence in the evolving stable boundary-layer, J. Atmos. Sci., 36, 1041–1052, 1979.

Chemel, C., Staquet, C., and Largeron, Y.: Generation of internal gravity waves by a katabatic wind in an idealized alpine valley, Meteorol. Atmos. Phys., 103, 187–194, 2009.

Chen, M., Talbot, R., Mao, H., Sive, B., Chen, J., and Griffin, R.J.: Air mass classification in coastal New England and its relationship to meteorological conditions, J. Geophys. Res., 112, D10S05, doi:10.1029/2006JD007687, 2007.

Chin, M., Jacob, D. J., Munger, J. W., Parrish, D. D., and Doddridge, B. G.: Relationship of ozone and carbon monoxide over North America, J. Geophys. Res., 99(D7), 14565–14573, 1994.

Contini, D., Cava, D., Martano, P., Donateo, A, and Grasso, F. M. :Comparison of indirect methods for the estimation of boundary layer height over flat-terrain in a coastal site, Meteorol. Z., 18(3), 309–320, 2009.

Cohen, R. A. and Kreitzberg, C. W.: Airstream boundaries in numerical weather simulations, Mon. Wea. Rev., 125, 168–183, 1997.

Collier, C. G., Davies, F., Bozier, K. E., Holt, A. R., Middleton, D. R., Pearson, G. N., Siemen, S., Willetts, D. V., Upton, G. J. G., and Young, R. I.: Dual-doppler lidar measurements for improving dispersion models, B. Am. Meteorol. Soc., 86, 825–838, 2005.

Cooper, D. I. and Eichinger, W. E.: Structure of the atmosphere in an urban planetary boundary-layer from lidar and radiosonde observations, J. Geophys. Res., 99(D11), 22937–22948, 1994.

Cooper, O. R., Moody, J. L., Parrish, D. D., Trainer,M., Ryerson, T. B., Holloway, J. S., Hubler, G., Fehsenfeld, F. C., Oltmans, S. J., and Evans, M. J.: Trace gas signatures of the airstreams within North Atlantic cyclones: Case studies from the North Atlantic Regional Experiment (NARE '97) aircraft intensive, J. Geophys. Res., 106, 5437–5456, 2001.

Cooper, O. R., Moody, J. L., Parrish, D. D., Trainer, M., Ryerson, T. B., Holloway, J. S., Hubler, G., Fehsenfeld, F. C., and Evans,M. J.: Trace gas composition of midlatitude cyclones over the western North Atlantic Ocean: A conceptual model, J. Geophys. Res., 107(D7), 4056, doi:10.1029/2001JD000901, 2002.

Cooper, O. R., Parrish, D. D., Stohl, A., Trainer, M., Nedelec, P., Thouret, V., Cammas, J. P., Oltmans, S. J., Johnson, B. J., Tarasick, D., Leblanc, T., McDermid, I. S., Jaffe, D., Gao, R., Stith, J., Ryerson, T., Aikin, K., Campos, T., Weinheimer A., and Avery, M. A.: Increasing springtime ozone mixing ratios in the free troposphere over western North America, Nature, 463, 344–348, 2010.

Corsmeier, U., Kalthoff, N., Kolle, O., Kotzian, M., Fiedler, F.: Ozone concentration jump in the stable nocturnal boundary layer during a LLJ-event. Atmospheric Environment 31, 1977–1989, 1997.

Craig, R. A., Measurements of temperature and humidity in the lowest 1000 ft of the atmosphere over Massachusetts Bay, Pap. Phys. Oceanogr. Meteorol., 10, 6-47, 1946.

Dacre, H. F., Gray, S. L., and Belcher, S. E.:, A case study of boundary layer ventilation by convection and coastal processes, J. Geophys. Res., 112, D17106, doi:10.1029/2006JD007984, 2007.

Darby, Lisa S., McKeen, S. A., Senff, C. J., White, A. B., Banta, R. M., Post, M. J., Brewer, W. A., Marchbanks, R. , Alvarez , R. J. II, Peckham, S. E., Mao, H. and Talbot, R.: Ozone differences between near-coastal and offshore sites in New England: Role of meteorology, J. Geophys. Res., 112, D16S91, doi:10.1029/2007JD008446, 2007.

Daum, P. H., Kleinman, L. I., Newman, L., Luke, W. T., Weinstein-Lloyd, J., Berkowitz, C. M., and Busness, K. M.: Chemical and physical properties of plumes of anthropogenic pollutants transported over the North Atlantic during the North Atlantic Regional Experiment, J. Geophys. Res., 101(D22), 29029–29042, doi:10.1029/95JD03163, 1996.

Day, D. A., Wooldridge, P. J., and Cohen, R. C.: Observations of the effects of temperature on atmospheric HNO3, SANs, SPNs, and NOx: evidence for a temperature-dependent HOx source, Atmos. Chem. Phys., 8, 1867–1879, doi:10.5194/acp-8-1867-2008, 2008.

Eckhardt, S., Stohl, A., Beirle, S., Spichtinger, N., James, P., Forster, C., Junker, C., Wagner, T., Platt, U., and Jennings, S. G.: The North Atlantic Oscillation controls air pollution transport to the Arctic, Atmos. Chem. Phys., 3, 1769-1778, doi:10.5194/acp-3-1769-2003, 2003.

Fairall, C. W., L. Bariteau, A. A. Grachev, R. J. Hill, D. E. Wolfe, W. A.Brewer, S. C. Tucker, J. E. Hare, and W. M. Angevine, Turbulent bulk transfer coefficients and ozone deposition velocity in the International Consortium for Atmospheric Research into Transport and Transformation, J. Geophys. Res., doi:10.1029/2006JD007597, 2006.

Fairall CW, Bradley EF, Hare JE, Grachev AA, Edson JB: Bulk parameterization of air-sea fluxes: updates and verification for the COARE algorithm. J Clim 16:571–591, 2003.

Fairall, C. W., Bariteau, L., Grachev, A. A., Hill, R. J., Wolfe, D. E., Brewer, W. A., Tucker, S. C., Hare, J. E., and Angevine,W. M.: Turbulent bulk transfer coefficients and ozone deposition velocity in the International Consortium for AtmosphericResearch into Transport and Transformation, J. Geophys. Res., 111, D23S20, doi:10.1029/2006JD007597, 2006.

Fehsenfeld, F. C., Ancellet, G., Bates, T. S., Goldstein, A. H., Hardesty, R. M., Honrath, R., Law, K. S., Lewis, A. C., Leaitch, R., McKeen, S., Meagher, J., Parrish, D. D., Pszenny, A. A. P., Russell, P. B., Schlager, H., Seinfeld, J., Talbot, R., and Zbinden, R.: International Consortium for Atmospheric Research on Transport and Transformation (ICARTT): North America to Europe—Overview of the 2004 summer field study, J. Geophys. Res., 111, D23S01, doi:10.1029/2006JD007829, 2006.

Flatoy, F., Hov, O., and Schlager, H.: Chemical forecasts used for measurement flight planning during POLINAT 2, Geophys. Res. Lett., 27, 951–954, 2000.

Forster, C., Cooper, O., Stohl, A., Eckhardt, S., James, P., Dunlea, E., Nicks Jr., D. K., Holloway, J. S., H"ubler, G., Parrish, D. D., Ryerson, T. B., and Trainer, M.: Lagrangian transport model forecasts and a transport climatology for the Intercontinental Transport and Chemical Transformation 2002 (ITCT 2k2) measurement campaign, J. Geophys. Res., 109, D07S92, doi:10.1029/2003JD003589, 2004.

Garratt, J. R.: The stably stratified internal boundary-layer for steady and diurnally varying offshore flow, Boundary Layer Meteorol., 38(4), 369–394, 1987.

Garratt, J.R., Ryan, B.F.: The Structure of the Stably Stratified Internal Boundary Layer in Offshore Flow over the sea. Boundary-Layer Meteorology 47, 17-40, 1989.

Garratt, J. R.: The internal boundary-layer—A review, Boundary Layer Meteorol., 50, 171– 203, 1990.

Gong, W., Mickle, R.E., Bottenheim, Foude, F., Beauchamp, S., Waugh, D.: Marine/coastal boundary layer and vertical structure of ozone observed at a coastal site in Nova Scotia during the 1996 NARSTO-CE field campaign, Atmos. Environ., 34, 4139-4154, 2000.

Gong, W., Lin, X., MeH nard, S., Pellerin, P., Benoit, R., Fehsenfeld, F.C., Daum, P., Leaitch, W.R., Trainer, M., Parrish, D.D., Hhbler, G. :Transport and processing of O3 and O3 precursors over the North Atlantic: an overview of the 1993 North

Atlantic Regional Experiment (NARE) summer intensive. J. Geophys. Res.101 D22, 1996.

Hanna, S. R.: The thickness of planetary boundary layer, Atmos.Environ., 3, 519–536, 1969.

Heard, D. E., Read, K. A., Methven, J., Al-Haider, S., Bloss, W. J., Johnson, G. P., Pilling, M. J., Seakins, P. W., Smith, S. C., Sommariva, R., Stanton, J. C., Still, T. J., Ingham, T., Brooks, B., De Leeuw, G., Jackson, A. V., McQuaid, J. B., Morgan, R., Smith, M. H., Carpenter, L. J., Carslaw, N., Hamilton, J., Hopkins, J. R., Lee, J. D., Lewis, A. C., Purvis, R. M., Wevill, D. J., Brough, N., Green, T., Mills, G., Penkett, S. A., Plane, J. M. C., Saiz-Lopez, A., Worton, D., Monks, P. S., Fleming, Z., Rickard, A. R., Alfarra, M. R., Allan, J. D., Bower, K., Coe, H., Cubison, M., Flynn, M., McFiggans, G., Gallagher, M., Norton, E. G., O'Dowd, C. D., Shillito, J., Topping, D., Vaughan, G., Williams, P., Bitter, M., Ball, S. M., Jones, R. L., Povey, I. M., O'Doherty, S., Simmonds, P. G., Allen, A., Kinnersley, R. P., Beddows, D. C. S., Dall'Osto, M., Harrison, R. M., Donovan, R. J., Heal, M. R., Jennings, S. G., Noone, C., and Spain, G.: The North Atlantic Marine Boundary Layer Experiment(NAMBLEX). Overview of the campaign held at Mace Head, Ireland, in summer 2002, Atmos. Chem. Phys., 6, 2241–2272, 2006.

Hojstrup, J.: Velocity spectra in the unstable planetary boundary layer, J. Atmos. Sci., 39, 2239–2248, 1982.

Holt, T. R. and Pullen, J.: Urban canopy modeling of the New York City metropolitan area: A comparison and validation of single- and multilayer parameterizations, Mon. Weather Rev., 135, 1906–1927, 2007.

Holton, J. R.: An Introduction to Dynamic Meteorology, 4th edn., Elsevier Academic Press, Burlington, 2004.

Holzworth: Estimates of mean maximum mixing depths in the contiguousUnited States, Mon. Weather Rev., 92, 235–242, 1964.

Hong, S.-Y., Dudhia, J., and Chen, S.-H.: A revised approach to ice microphysical processes for the bulk parameterization of cloud and precipitation, Mon. Weather Rev., 132, 103–120, 2004.

Honrath, R. E., Owen, R. C., Martin, M. V., Reid, J. S., Lapina, K., Fialho, P., Dziobak, M. P., Kleissl, J., and Westphal, D. L.: Regional and hemispheric impacts of anthropogenic and biomass burning emissions on summertime CO and O3 in the North Atlantic lower free troposphere., J. Geophys. Res., 109, D24310, doi:10.1029/2004JD005147, 2004.

Hsu, Shih-Ang: Coastal Meteorology.International Geophysics Series Academic Press, New York, 260 pp., 1988.

Hsu, S. A.: On the Growth of a Thermally Modified Boundary Layer by Advection of Warm Air over a Cooler Sea, J. Geophys. Res. 88(C1), 771-774. 1983

Hsu, S. A.: A Note on Estimating the Height of the Convective Internal Boundary Layer Near Shore, Bound. Layer Meteorol., 35, 311-316. 1987

Hsu, S. A.: A Verification of an Analytical Formula for Estimating the Height of the Stable Internal Boundary Layer, Bound. Layer Meteorol.,48, 197-201. 1989

Jacob, D., Crawford, J. H., Kleb, M. M., Connors, V. S., Bendura, R. J., Raper, J. L., Sachse, G. W., Gille, J. C., Emmons, L., and Heald, C. L.: Transport and Chemical Evolution over the Pacific (TRACE-P) aircraft mission: Design, execution, and first results, J. Geophys. Res., 108, 9000, doi:10.1029/2002JD003276, 2003.

Jacob, D. J., Logan, J. A., and Murti, P. P.: Effect of rising Asian emissions on surface ozone in the United States, Geophys. Res. Lett., 26, 2175–2178, 1999.

Jaffe, D., Anderson, T., Covert, D., Kotchenruther, R., Trost, B., Danielson, J., Simpson, W., Berntsen, T., Karlsdottir, S., Blake, D., Harris, J., Carmichael, G., and Uno, I.: Transport of Asian air pollution to North America, Geophys. Res. Lett., 26, 711– 714, 1999.

Johnson, D. W., Osborne, S., Wood, R., Suhre, K., Johnson, R., Businger, S., et al.: An overview of the Lagrangian experiments undertaken during the North Atlantic regional Aerosol Characterization Experiment (ACE-2), Tellus, 52B, 290–320, 2000.

Kaimal, J. C.: Horizontal velocity spectra in an unstable surface layer, J. Atmos. Sci., 35, 18–24, 1978.

Kaimal, J. C. and Finnigan, J. J.: Atmospheric Boundary Layer Flows: Their Structure and Measurement, Oxford University Press, UK, 1994.

Kaimal, J. C., Izumi, Y., Wyngaard, J. C., and Cote, R.: Spectral characteristics of surface-layer turbulence, Q. J. R. Meteorol. Soc., 98(417), 563–589, 1972.

Kaimal, J. C., Abshire, N. L., Chadwick, R. B., Decker, M. T., Hooke, W. H., Kropfli, R. A., Neff, W. D., and Pasqualucci, F.: Estimating the depth of the daytime convective boundary-layer, J. Appl. Meteorol., 21, 1123–1129, 1982.

Kalnay, E., Kanamitsu, M., Kistler, R., Collins, W., Deaven, D., Gandin, L., Iredell, M., Saha, S., White, G., Woollen, J., Zhu, Y., Chelliah, M., Ebisuzaki, W., Higgins, W., Janowiak, J., Mo,K. C., Ropelewski, C., Wang, J., Leetmaa, A., Reynolds,

R.,Jenne, R., and Joseph, D.: The NCEP/NCAR Reanalysis 40-year Project, Bull. Amer. Meteor. Soc., 77, 437–471, 1996.

Kerr, D. E., Propagation of Short Radio Waves, McGraw-Hill, New York, 1951.

Kitaigorodskii, S. A. and Joffre, S. M.: In search of a simple scaling for the height of the stratified atmospheric boundary layer, Tellus A, 40A, 419–433, 1988.

Kleinman, L. I., Springston, S. R., Daum, P. H., Lee, Y.-N., Nunnermacker, L. J., Senum, G. I., Wang, J., Weinstein-Lloyd, J.,Alexander, M. L., Hubbe, J., Ortega, J., Canagaratna, M. R., and Jayne, J.: The time evolution of aerosol composition over the Mexico City plateau, Atmos. Chem. Phys., 8, 1559–1575, doi:10.5194/acp-8-1559-2008, 2008.

Kundu, P.K and Cohen, I.M.: Fluid Mechanics, Second Edition. San Diego: Academic Press, 730 pp., 1990.

Lawrence, M. G., Rasch, P. J., von Kuhlmann, R., Williams, J., Fischer, H., de Reus, M., Lelieveld, J., Crutzen, P. J., Schultz, M., Stier, P., Huntrieser, H., Heland, J., Stohl, A., Forster, C., Elbern, H., Jakobs, H., and Dickerson, R. R.: Global chemical weather forecasts for field campaign planning: predictions and observations of large-scale features during MINOS, CONTRACE and INDOEX, Atmos. Chem. Phys., 3, 267–289, 2003.

Lee, A. M., Carver, G. D., Chipperfield, M. P., and Pyle, J. A.: Three-dimensional chemical weather forecasting: A Methodology, J. Geophys. Res., 102, 3905–3919, 1997.

Lee, S.-H., McKeen, S. A., Angevine, W. M., Frost, G. J., Kim, S.-W., and Trainer, M.: Impact of an urban land surface parameterization on the transport and dispersion of gaseous air pollutant, The 7th International Conference on Urban Climate, Yokohama, Japan, 29 June–3 July, 2009.

Lenschow, D. H. and Stankov, B. B.: Length scales in the convective boundary-layer, J. Atmos. Sci., 43, 1198–1209, 1988.

Li, Q., Jacob, D. J., Bey, I., Palmer, P. I., Duncan, B. N., Field, B. D., Martin, R. V., Fiore, A. M., 20 Yantosca, R. M., Parrish, D. D., Simmonds, P. G., and Oltmans, S. J.: Transatlantic transportof pollution and its effects on surface ozone in Europe and North America, J. Geophys. Res., 107(D13), 4166, doi:10.1029/2001JD001422, 2002.

Li, Q., Jacob, D. J., Park, R., Wang, Y., Heald, C. L., Hudman, R., Yantosca, R. M., Martin, R. V., and Evans, M.: North American pollution outflow and the trapping of convectively lifted pollution by upper-level anticyclone, J. Goephys. Res., 110, D10301, doi:10.1029/2004JD005039, 2005.

Liu, X. H. and Ohtaki, E.: An independent method to determine the height of the mixed layer, Bound.-Lay. Meteorol., 85, 497–504,1997.

Mahrt, L., Heald, R.C., Lenschow, D.H., Stankov, B.B.: An observational study of the structure of the nocturnal boundary layer. Boundary-Layer Meteorology 17, 247–264. 1979.

Mahrt, L.: Vertical structure and turbulence in the very stable boundary layer. Journal of the Atmospheric Sciences, 42, 2333–2349, 1985.

Mahrt, L.: Vertical Structure and Turbulence in the Very Stable Boundary Layer, J. Atmos. Sci. 42, 2333–2349, 1985.

Mao, H., and Talbot, R.: Relationship of surface O_3 to large-scale circulation patterns during two recent winters, Geophys. Res. Lett., 31(6), L06108, 10.1029/2003GL018860, 2004a.

Mao, H., and Talbot,R.:, O_3 and CO in New England: Temporal variations and relationships, J. Geophys. Res., 109, D21304, doi:10.1029/2004JD004913, 2004b.

Mao, H., Talbot, R., Troop, D., Johnson, R., Businger, S., and Thompson, A. M.: Smart balloon observations over the North Atlantic: O3 data analysis and modeling, J. Geophys. Res., 111, D23S56, doi:10.1029/2005JD006507, 2006.

Methven, J., Arnold, S. R., Stohl, A., Avery, M., Law, K., Lewis, A., Parrish, D., Reeves, C., Schlager, H., Atlas, E., Blake, D., and Rappengluck, B.: Establishing Lagrangian connections between observations within air masses crossing the Atlantic during the ICARTT experiment, J. Geophys. Res., 111, D23S62, doi:10.1029/2006JD007540, 2006.

Millet, D. B., Goldstein, A. H., Holzinger, R., Williams, B. J., Allan, J. D., Jimenez, J. L., Worsnop, D. R., Roberts, J. M., White, A. B., Hudman, R. C., Bertschi, I. T., and Stohl, A.: Chemical characteristics of North American surface layer outflow: Insights from Chebogue Point Nova Scotia, J. Geophys. Res., 111, D23S53, doi:10.1029/2006JD007287, 2006.

Mulhearn, P. J., On the formation of a stably stratified internal boundary layer by advection of warm air over a cooler sea, Boundary Layer Meteorol., 21, 247-254, 1981.

Mulhearn, P. J.: Turbulent Boundary Layer Wall-Pressure Fluctuations Downstream of an Abrupt Change in Surface Roughness, Phys. Fluids 19, 796-801. 1976.

Mulhearn, P. J.: Relations between Surface Fluxes and Mean Profiles of Velocity, Temperature, and Concentration, Downwind of a Change in Surface Roughness, Quart. J. Roy. Meteorol. Soc.103, 785-802. 1977.

Mulhearn, P. J.: A Wind-Tunnel Boundary-Layer Study of the Effects of a Surface Roughness Change; Rough to Smooth, Boundary-Layer Meteorol. 15, 3-30. 1978.

Mulhearn, P. J.: On the Formation of a Stably Stratified Internal Boundary Layer by Advection of Warm Air over a Cooler Sea, Boundary-Layer Meteorol. 21, 247-254. 1981.

Neuman, J. A., Parrish, D. D., Trainer, M., Ryerson, T. B., Holloway, J. S., Nowak, J. B., Swanson, A., Flocke, F., Roberts, J. M., Brown, S. S., Stark, H., Sommariva, R., Stohl, A., Peltier, R., Weber, R., Wollny, A. G., Sueper, D. T., Hubler, G., and Fehsenfeld, F. C.: Reactive nitrogen transport and photochemistry in urban plumes over the North Atlantic Ocean, J. Geophys. Res., 111, D23S54, doi:10.1029/2005JD007010, 2006.

Owen, R. C., Cooper, O. R., Stohl, A., and Honrath, R. E.: An analysis of the mechanisms of North American pollutant transport to the central North Atlantic lower free troposphere., J. Geophys. Res., 111, D23S58, doi:10.1029/2006JD007062, 2006.

Panofsky, H. A., Tennekes, H., Lenschow, D. H., and Wyngaard, J. C.: The characteristics of turbulent velocity components in the surface layer under convective conditions, Bound.-Lay. Meteorol.,11, 355–361, 1977.

Panofsky, H. A., Larko, D., Lipschutz, R., Stone, G., Bradley, E. F., Bowen, A. J., and Hojstrup, J., Spectra of velocity components over complex terrain, Q. J. R. Meteorol. Soc., 108, 215–230, 1982.

Panofsky, H. A. and Dutton, J. A.: Atmospheric Turbulence: Models and Methods for Engineering Applications, John Willey & Sons, Inc., New York, 1984.

Parrish, D. D., Holloway, J. S., Trainer, M., Murphy, P. C., Forbes, G. L., and Fehsenfeld, F. C.: Export of North American Ozone Pollution to the North Atlantic Ocean, Science, 259(5100),1436–1439, 1993.

Real, E., Law, K. S., Schlager, H., Roiger, A., Huntrieser, H., Methven, J., Cain, M., Holloway, J., Neuman, J. A., Ryerson, T., Flocke, F., de Gouw, J., Atlas, E., Donnelly, S., and Parrish, D.: Lagrangian analysis of low altitude anthropogenic plume processing across the North Atlantic, Atmos. Chem. Phys., 8, 7737-7754, 2008.

Renfrew, I. A. and J. C. King: A simple model of the convective internal boundary layer and its application to surface heat flux estimates within polynyas, Boundary-Layer Meteorol., 94, 335-356, 2000.

Roll, H., Physics of the Marine Boundary Layer, Academic Press Inc. New York, 425pp, 1965.

Rowe, M. J. Perlinger, C. Fairall: A Lagrangian model to predict the modification of near-surface scalar mixing ratios and air–water exchange fluxes in offshore flow, Boundary-Layer Meteorol., 140, 87-103, doi:10.1007/s10546-011-9598-0, 2011.

Samson, P.J.: Nocturnal ozone maxima. Atmospheric Environment 12, 951–955, 1978.

Seinfeld, J. H. and Pandis, S. N.: Atmospheric chemistry and physics, Wiley, New York, 1998.

Simmonds, P. G., Derwent, R. G., Manning, A. L., and Spain,G.: Significant growth in surface ozone at Mace Head, Ireland, 1987– 2003,Atmos. Environ., 38, 4769–4778. 2003.

Slowik, J. G., Brook, J., Chang, R. Y.-W., Evans, G. J., Hayden, K., Jeong, C.-H., Li, S.-M., Liggio, J., Liu, P. S. K., McGuire, M., Mihele, C., Sjostedt, S., Vlasenko, A., and Abbatt, J. P. D.: Photochemical processing of organic aerosol at nearby continental sites: contrast between urban plumes and regional aerosol, Atmos. Chem. Phys., 11, 2991-3006, doi:10.5194/acp-11-2991-2011, 2011.

Smedman, A.-S., Bergstrom, H. and Hogstrom, U. : Spectra, variances and length scales in a marine stable boundary layer dominated by a low level jet. Boundary-Layer Meteorol. 76, 211–232. 1995.

Smedman, A.-S., Bergström, H. and Grisogono, B.: Evolution of stable internal boundary layers over a cold sea, J. Geophys. Res., 102(C1), 1091–1099, doi:10.1029/96JC02782, 1997.

Stohl, A., Hittenberger, M., and Wotawa, G.: Validation of the Lagrangian particle dispersion model FLEXPART against large scale tracer experiment data, Atmos. Environ., 32, 4245–4264, 1998.

Stohl, A. and Thomson, D. J.: A density correction for Lagrangian particle dispersion models, Boundary-Layer Meteorol., 90, 155– 167, 1999.

Stohl, A., and Trickl, T.: A textbook example of long-range transport: Simultaneous observation of ozone maxima of stratospheric and North American origin in the free troposphere over Europe, J. Geophys. Res., 104, 30,445– 30,462, 1999.

Stohl, A.: A one-year Lagrangian "climatology" of air streams in the northern hemisphere troposphere and lowermost stratosphere, J. Geophys. Res., 106, 7263–7279, 2001.

Stohl, A., Eckhardt, S., Forster, C., James, P., and Spichtinger, N.: On the pathways and timescales of intercontinental air pollution transport, J. Geophys. Res., 107, 4684, doi:10.1029/2001JD001396, 2002.

Stohl, A., Eckhardt, S., Forster, C., James, P., Spichtinger, N., and Seibert, P.: A replacement for simple back trajectory calculations in the interpretation of atmospheric trace substance measurements, Atmos. Environ., 36, 4635–4648, 2002.

Stohl, A., Trainer, M., Ryerson, T., Holloway, J., and Parrish, D.: Export of NOy from the North American boundary layer during NARE 96 and NARE 97, J. Geophys. Res., 107, 4131, doi:10.1029/2001JD000519, 2002.

Stohl, A., Forster, C., Eckhardt, S., Spichtinger, N., Huntrieser, H., Heland, J., Schlager, H.,Wilhelm, S., Arnold, F., and Cooper, O.: A backward modeling study of intercontinental pollution transport using aircraft measurements, J. Geophys. Res., 108, 4370, doi:10.1029/2002JD002862, 2003.

Stull, R.B.: An Introduction to Boundary Layer Meteorology, Dordrecht, Kluwer Academic, 683 p., 1988.

Sullivan, P. P., Moeng, C. H., Stevens, B., Lenschow, D. H., and Mayor, S. D.: Structure of the entrainment zone capping the convective atmospheric boundary layer, J. Atmos. Sci., 55, 3042–3064, 1998.

Sutton, 0. G.: Wind Structure and Evaporation in a Turbulent Atmosphere, Proc. Roy. Soc. (London), Ser. A, 146, 701-722, 1934.

Sutton, 0. G.: Micrometeorology, McGraw-Hill, New York, 333 pp. 1953.

Tardif, R. and Rasmussen, R. M.: Process-oriented analysis of environmental conditions associated with precipitation fog events in the New York City region. J. Appl. Meteor. Climatol. 005, 2007.

Taylor, G. I.: The spectrum of turbulence, Proc. Roy. Soc. A, 164,476–490, 1938.

Thompson, A. M., Stone, J. B., Witte, J. C., Miller, S. K., Pierce, R. B., Chatfield, R. B., Oltmans, S. J., Cooper, O. R., Loucks, A. L., Taubman, B. F., Johnson, B. J., Joseph, E., Kucsera, T. L., Merrill, J. T., Morris, G. A., Hersey, S., Forbes, G., Newchurch, M. J., Schmidlin, F. J., Tarasick, D. W., Thouret, V., and Cammas J.-P.: Intercontinental chemical transport experiment ozonesonde network study (IONS) 2004: 1. Summertime upper troposphere/lower stratosphere ozone over

northeastern North America, J. Geophys. Res., 112, D12S12, doi:10.1029/2006JD007441, 2007.

Trainer, M., Ridley, B. A., Buhr, M. P., Kok, G., Walega, J., Hubler, G., Parrish, D. D., and Fehsenfeld, F. C.: Regional ozone and urban plumes in the southeastern United States: Birmingham, a case study, J. Geophys. Res., 100(D9), 18823–18834, 1995. Turquety, S., Logan, J. A., Jacob, D. J., Hudman, R. C., Leung, F. Y., Heald, C. L., Yantosca, R. M., Wu, S., Emmons, L. K., Edwards, D. P., and Sachse, G.W.: Inventory of boreal fire emissions for North America in 2004: Importance of peat burning and pyroconvective injection, J. Geophys. Res., 112, D12S03, doi:10.1029/2006JD007281, 2007.

Trickl, T., Cooper, O. R., Eisele, H., James, P., Mucke, R., and Stohl, A.: Intercontinental transport and its influence on the ozone concentrations over central Europe: Three case studies, J. Geophys. Res., 108(D12), 8530, doi:10.1029/2002JD002735, 2003.

Verver, G. H. L., Van Dop, H., and Holtslag, A. A. M.: Turbulent mixing of reactive gases in the convective boundary layer, Bound.-Layer Meteorol., 85, 197–222, 1997.

Vesala, T., Jarvi, L., Launiainen, S., Sogachev, A., Rannik, U., Mammarella, I., Siivola, E., Keronen, P., Rinne, J., Riikonen,A. and Nikinmaa, E.: Suface-atmosphere interactions over complexurban terrain in Helsinki, Finland, Tellus B – Chem. Phys.Meteorol., 60(2), 188–189, 2008.

Wang, H., Jacob, D. J., Le Sager P., Streets, D. G., Park, R. J., Gilliland, A. B., and van Donkelaar, A.: Surface ozone background in the United States: Canadian and Mexican pollution influences, Atmos. Environ., 43, 1310–1319, 2009a.

Wang, H., Skamarock,W. C., and Feingold, G.: Evaluation of scalar advection schemes in the Advanced Research WRF model using large-eddy simulations of aerosol-cloud interactions, Mon. Weather Rev., 137, 2547–2558, 2009b.

Ward, E., Susott, R., Kaufman, J., Babbit, R., Cummings, D., Dias, B., Holben, B., Kaufman, Y., Rasmussen, R., and Setzer, A.: Smoke and fire characteristics for cerrado and deforestation burns in Brazil: BASE-B experiment, J. Geophys. Res., 97(D13), 14601–14619, 1992.

Warneke, C., de Gouw, J. A., Goldan, P. D., Kuster, A. C.,Williams, E. J., Lerner, B. M., Jakoubek, R., Brown, S. S., Stark, H., Aldener, M., Ravishankara, A. R., Roberts, J. M., Marchewka, M., Bertman, S., Sueper, D. T., McKenne, S. A., Meagher, J. F., and Feshenfeld, F. C.: Comparison of daytime and nightime oxidation of biogenic VOCs along the New England coast in summer during New England Air Quality Study 2002., J. Geophys. Res., 109, D10309, doi:10.1029/2003JD004424,

2004. Wentz, F. J. and Spencer, R. W.: SSMI/I rain retrievals within a unified all-weather ocean algorithm, J. Atmos. Sci., 55, 1149–1152, 1998.

Wilczak, J. M., Oncley, S. P., and Stage, S. A.: Sonic anemometer tilt correction algorithms, Bound.-Layer Meteorol., 99, 127–150, 2001.

Wild, O. and Akimoto, H.: Intercontinental transport of ozone and its precursors in a three-dimensional global CTM, J. Geophys. Res., 106, 27 729–27 744, 2001.

Wood, C. R., Lacser, A., Barlow, J. F., Padhra, A., Belcher, S. E.,Nemitz, E., Helfter, C., Famulari, D., and Grimmond, C. S. B.:Turbulent flow at 190 metres above London during 2006–2008:a climatology and the applicability of similarity theory, Bound.-Layer Meteorol., 137, 77–96, 2010

Wu, X. and Zhang, J.: Instability of a stratified boundary layer and its coupling with internal gravity waves. Part 1. Linear and nonlinear instabilities, J. Fluid Mech., 595, 379–408, 2008.

Wyngaard, J. C. and Lemone, M. A.: Behavior of the refractive index structure parameter in the entraining convective boundary- layer, J. Atmos. Sci., 37, 1573–1585, 1980.

Wyngaard, J. C.: Structure of the PBL in Lectures on air pollution modeling, edited by: Venkatram, A., andWyngaard, J. C., American Meteorological Society, Boston, USA, 1988.

Wyngaard, J. C.: Turbulence in the atmosphere, Cambridge University Press, Cambridge, UK, 2010.

Zeng, X. B., Brunke, M. A., Zhou, M. Y., Fairall, C., Bond, N. A.,and Lenschow, D. H.: Marine atmospheric boundary layer height over the eastern Pacific: Data analysis and model evaluation, J. Climate, 17, 4159–4170, 2004.

Zhou, Y., Mao, H., Russo, R. S., Blake, D. R., Wingenter, O. W., Haase, K. B., Ambrose, J., Varner, R. K., Talbot, R., and Sive, B. C.: Bromoform and dibromomethane measurements in the seacoast region of New Hampshire 2002–2004, J. Geophys. Res.,113, D08305, doi:10.1029/2007JD009103, 2008.

Zilitinkevich, S. S.: On the determination of the height of the Ekman boundary layer, Bound.-Lay. Meteorol., 3, 141–145, 1972.

Zilitinkevich, S., Esau, I., and Baklanov, A.: Further comments on the equilibrium height of neutral and stable planetary boundary layers, Q. J. R. Meteorol. Soc., 133, 265–271, doi:10.1002/qj.27, 2007.

Zilitinkevich, S. S., Elperin, T., Kleeorin, N., L'Vov, V., and Rogachevskii, I.: Energy- and Flux-Budget Turbulence Closure Model for Stably Stratified Flows, Part II: The Role of Internal Gravity Waves, Bound.-Lay. Meteorol., 133, 139–164, doi:10.1007/s10546-009-9424-0, 2009.